Tartu University

Faculty of Science and Technology

Institute of Technology

Oliver Vaht

Design and Characterization of an Ultra-Wideband Radio for Extended-Range Transmission

Master's thesis (30 EAP)
Robotics and Computer Engineering

Supervisor:

Jaanus Kalde

Tartu 2025

Abstract

Design and Characterization of an Ultra-Wideband Radio for Extended-Range Transmission

This thesis presents the design and characterization of a custom ultra-wideband radio system for extended-range communication. Existing commercial modules were found inadequate due to limited configurability and restricted frequency range. To overcome these issues, a UWB platform was developed, including a transceiver based on the DW1000 chip, a power amplifier using the Renesas F1485, and a pentagon-shaped antenna optimized for 3–5 GHz.

All components were validated through measurements. Field tests were conducted in real outdoor conditions with a special frequency license. Maximum communication distance achieved was 2.63 km using UWB Channel 4. Bit error rate remained low, with packet loss becoming the main limiting factor at longer ranges.

The results show that with custom hardware and correct configuration, UWB can be used effectively for extended-range transmission in real-world conditions.

CERCS: T170 Electronics; T191 High frequency technology, microwaves.

Keywords: Electronics, Ultra-Wideband Radio, Radio-frequency engineering.

Resümee

Ultralairiba raadio projekteerimine ja iseloomustamine kõrgendatud sideks

Käesolev magistritöö käsitleb ultralairiba raadiosüsteemi projekteerimist ja iseloomustamist kõrgendatud side jaoks. Olemasolevad turul saadavad moodulid osutusid ebasobivaks piiratud seadistamisvõimaluste, sagedusvahemiku ja halva signaali kvaliteedi tõttu. Nende puuduste ületamiseks töötati välja ultralairiba platvorm, mis koosneb DW1000 kiibil põhinevast saatja-vastuvõtja plaadist, Renesas F1485 põhinevast võimendist ning 3–5 GHz sagedusvahemikule optimeeritud viisnurksest antennist.

Kõik komponendid valideeriti mõõtmiste abil. Välitestid viidi läbi reaalsetes välistingimustes spetsiaalse sagedusloa alusel. Maksimaalseks sideulatuvuseks mõõdeti 2,63 km, kasutades UWB kanalit 4. Bitiveateguri määr jäi madalaks, kuid pikematel distantsidel sai paketikadu peamiseks piiravaks teguriks.

Tulemused näitavad, et kohandatud riistvara ja korrektse seadistusega on UWB tehnoloogia tõhus vahend pikamaa andmesideks reaalses keskkonnas.

CERCS: T170 Elektroonika; T191 Kõrgsagedustehnoloogia, mikrolained.

Märksõnad: Elektroonika, Ultralairiba raadio, Raadiosagedustehnika.

Contents

List of Figures

List of Tables

Abbreviations, constants, definitions

API Application Programming Interface

BER Bit Error Rate

BOM Bill of Materials

dB Decibel — logarithmic unit for signal gain or loss

dBm Decibel-milliwatts — absolute power level referenced to 1 mW

EOL End of Life (product lifecycle)

FCS Frame Check Sequence

GPS Global Positioning System

LED Light Emitting Diode

LNA Low-Noise Amplifier

LoS Line of Sight

m Meter — SI unit of distance

PCB Printed Circuit Board

PDoA Phase Difference of Arrival

PRF Pulse Repetition Frequency

RF Radio Frequency

RTK Real Time Kinematic

SFD Start Frame Delimiter

SPI Serial Peripheral Interface

TDoA Time Difference of Arrival

TWR Two-Way Ranging

UWB Ultra-Wideband

UPS Uninterruptible Power Supply

USB Universal Serial Bus

1 Introduction

Reliable localization remains a key challenge in industries such as autonomous driving, robotics and logistics[1][2][3]. Although GPS is widely used for outdoor positioning, it is limited by interference, multipath effects, attenuation, and recently deliberate jamming[4][5], highlighting the need for alternatives.

Ultrawideband radio technology emerges as a promising candidate due to its high temporal resolution, precise ranging capabilities, and resistance to multipath effects[6]. Although UWB-based localization has mostly been demonstrated in controlled indoor environments, its reliability and performance in real-world conditions has not been researched that much[7][8][9][10].

This thesis aims to address this gap by validating the feasibility of using ultrawideband radio technology for localization under realistic outdoor scenarios. The primary goal is to clearly define the system and assess if UWB can be used outdoors. Specifically, this work will measure maximum communication range, characterize bit-error rates as a function of distance and compare performance across multiple UWB channels. The outcomes are intended to provide practical insights for future research on robust, long-range UWB usage.

2 Overview of Localization and UWB Radio Technology

2.1 Relevance and Importance of Localization

Localization, in robotics, refers to the robot's ability to accurately determine its position and orientation within a given environment [1]. Precise localization is fundamental for numerous tasks, notably path planning, where the robot's current position and the target destination define a trajectory.

Although the concept of navigating from point A to point B is intuitively simple, is practice this requires addressing several variables, such as environmental conditions and robot-specific characteristics. Autonomous vehicles exemplify this complexity: despite substantial financial investment, fully autonomous driving systems have not yet been realized [11], [12].

Localization is crucial as it provides the capability required for autonomous operation. Accurate knowledge of the robot's position enables decision-making, such as obstacle avoidance, thereby enhancing task safety. The greater the precision in determining the robot's position, the more efficiently and reliably the robot can execute its task[13].

2.2 Current Solutions and their Limitations

Several technologies are currently used to achieve reliable localization, each with distinct strengths and limitations[13]:

Global Positioning System (GPS): GPS is extensively employed for outdoor localization, providing global positioning information for robots and autonomous systems. Despite its widespread use, GPS accuracy significantly diminishes in urban or indoor environments due to interference, multipath propagation, signal attenuation, and deliberate jamming [14]. Enhancements such as Real-Time Kinematic (RTK) GPS can improve positional accuracy, but with a low polling rate [15].

LiDAR (Light Detection and Ranging): LiDAR sensors offer high-resolution, three-dimensional mapping of surrounding environments, allowing for accurate localization by detecting and classifying obstacles and landmarks. Nevertheless, LiDAR systems are generally costly, computationally demanding, and sensitive to adverse weather conditions, such as rain, fog, or dust, which can compromise sensor performance and accuracy[16].

Visual Odometry: This method utilizes image data captured by cameras to estimate robot

motion and position. By applying computer vision algorithms analyzing consecutive images, visual odometry can provide precise localization. However,its dependent on environmental conditions, such as lighting and texture richness[13].

Each of these technologies has specific contexts in which they excel, as well as scenarios where their limitations become highly relevant. In demanding localization scenarios, combining multiple technologies, such as GPS, LiDAR, and visual odometry, can provide robust and accurate localization solutions by compensating for each method's individual weaknesses. Tabel 2.1 brings out each technologies strenghts, limitations, accuracy, cost and robustness.

Table 2.1: Comparison of GPS, LiDAR, and Visual Odometry

Technology	**Strengths**	**Limitations**	**Accuracy**	**Cost**	**Robustness**
GPS	Global coverage, ideal outdoors	Affected by interference, multipath, jamming	Moderate to High	Low to Moderate	Poor (urban/indoor)
LiDAR	High-res 3D mapping, precise localization	Costly, weather-sensitive, compute-heavy	High	High	Moderate to Poor
Visual Odometry	Accurate motion from visual data	Sensitive to lighting, compute-heavy	Moderate to High	Moderate	Moderate (lighting dependent)

Sources: [13], [14], [16]

2.3 Introduction to Ultra-Wideband

Considering the previously discussed limitations associated with conventional localization methods it is evident that alternative technologies are necessary. UWB technology emerges as a promising solution that addresses many of these challenges.

UWB uses very short-duration pulses spread over a wide frequency spectrum. Conventional radio technologies use narrow frequency bands, whereas UWB's short pulses occupy a broader portion of the radio spectrum. These pulses occupy a wide bandwidth because, mathematically, the shorter a pulse in time, the wider its frequency spectrum. This is a direct consequence of the Fourier transform relationship between time and frequency.

UWB achieves precise positioning by accurately measuring the Time-of-Flight (ToF) of its short-duration pulses. Due to their brief duration, these pulses allow the receiver to measure the arrival time with very high precision, which directly improves the accuracy of the calculated distance. In comparison, narrowband signals have longer pulses, which limits their temporal resolution and reduces positioning precision.

Multipath interference occurs when a transmitted signal reaches the receiver through multiple paths, typically due to reflections. Narrowband signals overlap significantly with their reflections, complicating signal detection and reducing positioning accuracy. UWB's short pulses, however, clearly separate the direct signal from reflected signals because the reflections arrive later in time. This clear separation allows the receiver to identify and use only the first arriving signal for distance measurement, effectively reducing multipath-related errors.[17], [18]

Figure 2.1 illustrates the use ToF for distance estimation in an indoor environment. An UWB signal transmitted by the blue device reaches the green device through multiple propagation paths. One path is direct, passing through walls, while others are longer due to reflections. The shortest path arrives first and is used to compute the ToF. Reflected signals are discarded. The principle is comparable to selecting the first finisher in a race.**noauthor_getting_nodate**

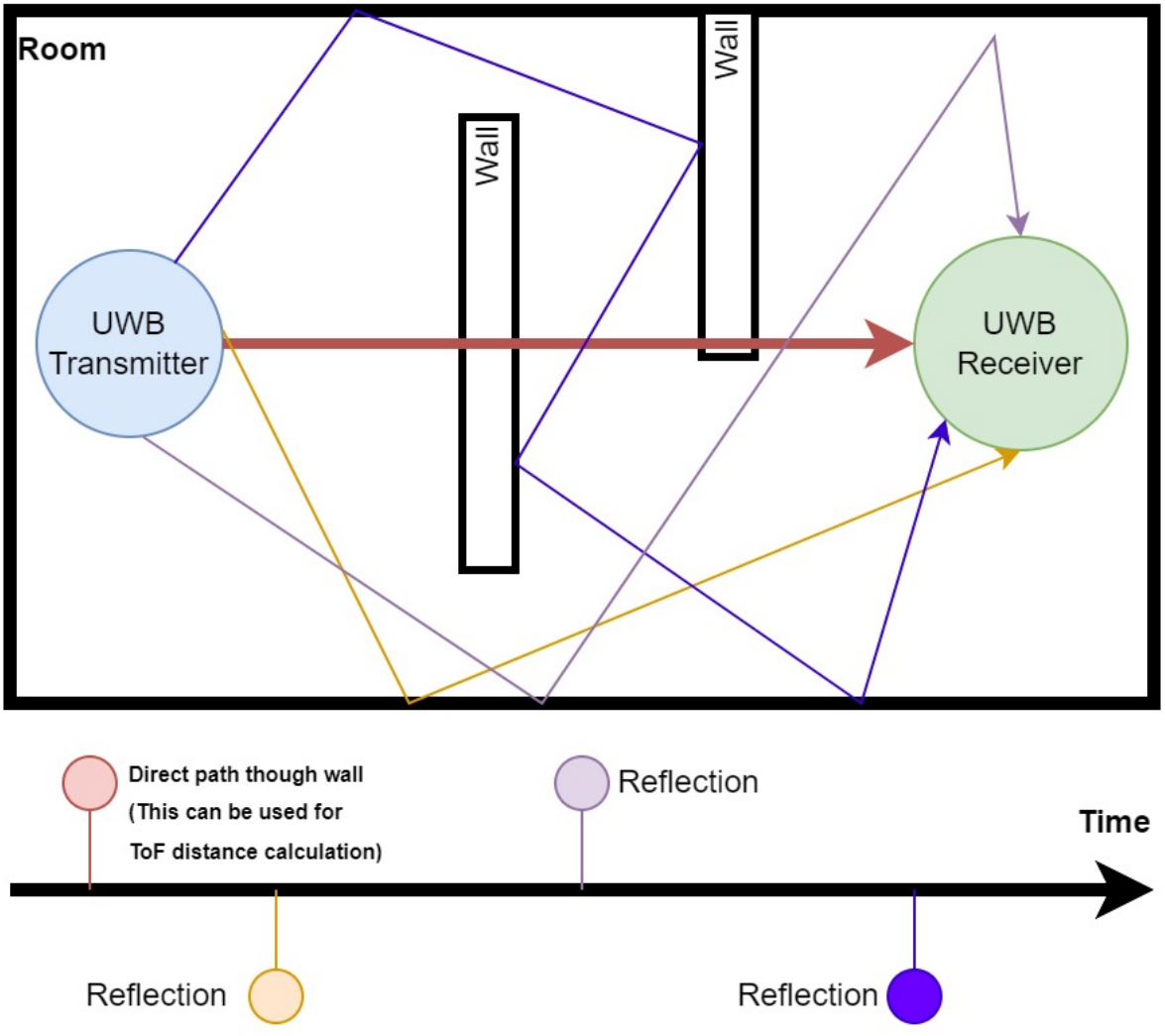

Figure 2.1: Propagation of UWB signal in space

UWB-based localization relies on precise ToF measurements, where distance is calculated by multiplying signal travel time by the speed of light. Three main ToF-based ranging techniques are used:

- **Time Difference of Arrival (TDoA)**: Similar to GPS, multiple synchronized receivers timestamp incoming signals from transmitter, and a central system computes device positions through multilateration. This technique is suited to scenarios requiring high device density and low power consumption but demands synchronized receivers. Figure 2.2 illustrates the workings of the TDoA.

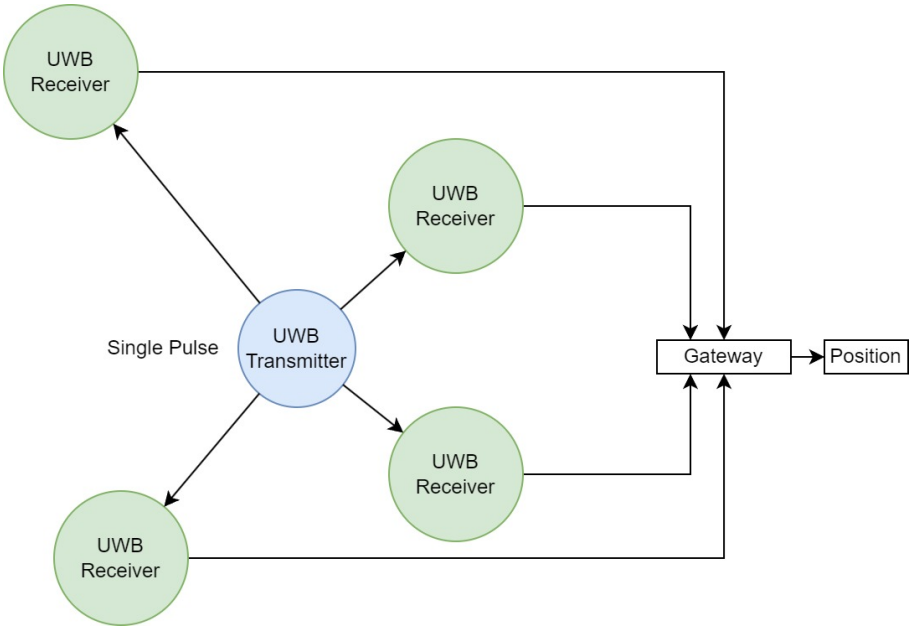

Figure 2.2: Time Difference of Arrival

- **Two-Way Ranging (TWR)**: Devices actively communicate with each other, measuring the round-trip signal travel time. This method allows for easy deployment without system-wide synchronization and allows data exchange, though it involves higher power consumption and supports fewer devices. Figure 2.3 illustrates the workings of the TWR.

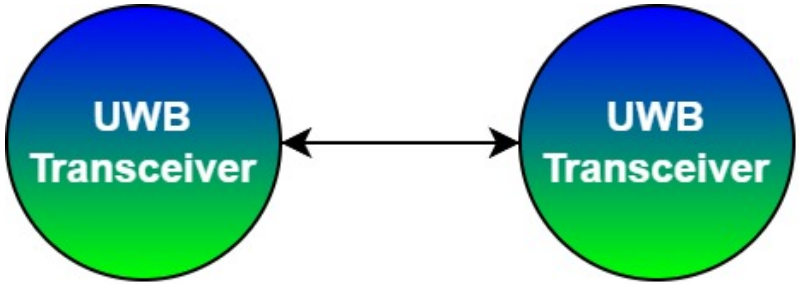

Figure 2.3: Two-Way Ranging

- **Phase Difference of Arrival (PDoA)**: Combines TWR distance measurement with directional bearing through phase difference measurements across multiple antennas on a single device. PDoA reduces the infrastructure needed but introduces positioning errors proportional to the distance between devices. Figure 2.4 illustrates the workings of the PDoA.

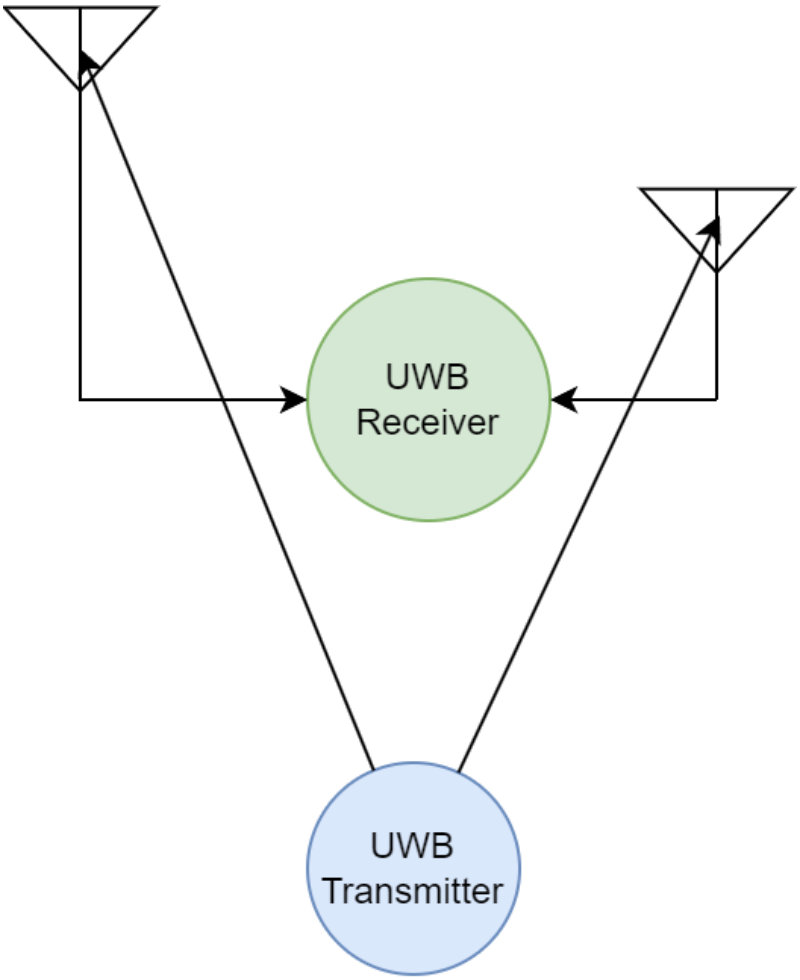

Figure 2.4: Phase Difference of Arrival

2.4 Research on UWB Radio

Despite the promising theoretical capabilities of UWB, practical studies remain limited, particularly under real-world outdoor conditions. This section analyzes literature to assess the state of UWB based localisation.

- **Rykała et al.** [8] propose a UWB-based outdoor localization system for UGVs using the Decawave TREK1000 and test trilateration, NLP, and geometric methods. Algorithms adapt to available sensor data and perform well outdoors, but the study omits key parameters like anchor spacing, signal thresholds, and performance limits, hindering reproducibility and comparison.

- **Xia et al.** [9] report about the development of a 3–5 GHz impulse radio UWB transmitter and receiver MMIC optimized for long-range precision wireless sensor networks. Their system achieves ranging accuracy better than 15 cm up to 200 m line-of-sight (LOS) outdoors using TDoA measurements and high-peak-power UWB pulses (20 dBm). While the achieved range is impressive, the conditions that outdoor tests are conducted are

not mentioned. Also no mention of antenna radiation efficiency is mentioned only the omnidirectionality.

- **Van Herbruggen et al.** [10] propose Wi-PoS, a low-cost, open-source UWB hardware platform equipped with sub-GHz and 2.4 GHz back-end communication. Their work combines hardware design and protocol stack integration with a focus on deployability and energy efficiency. In outdoor field tests, the system achieved sub-5 cm accuracy at 50 m and 75 m distances using TWR and RTK-assisted calibration. The hardware used was Decawave DW1000 transceivers.

In summary, while all three studies demonstrate the practical potential of UWB-based systems in outdoor settings, there remains a lack of detailed performance characterization. This necessitates the need for further systematic testing and parameterized evaluations of UWB radio performance in outdoor environments.

3 Purpose of Work

The objective of this thesis is to develop and empirically characterize a UWB radio system capable for achieving the maximum possible communication distance in real-world conditions.

4 Methodology

4.1 Overview and Objectives

The objective is to experimentally validate the feasibility of using UWB technology for extended-range applications. To achieve this, existing solutions, including commercially available UWB modules, amplifiers, and antennas, are assessed to prevent redundant development efforts. Each component is evaluated quantitatively, with performance metrics clearly described.

4.2 System Overview and Architecture

Figure 4.1 illustrates a suitable architecture for evaluating UWB radio performance in extended-range scenarios. Given that the primary objective is to measure achievable signal range, the architecture is designed to possibly allow each radio board to function either as a transmitter (TX) or receiver (RX). Although the inclusion of an RF switch could enable half-duplex communication within a single module, such implementation lies beyond the scope of this thesis.

Figure 4.1: Proposed architecture for TX side UWB radio testing.

This architecture is modular and easily adaptable. During the design phase, the potential addition of a Low Noise Amplifier (LNA) was evaluated if deemed necessary. The finalized receiver-side architecture utilized in this thesis is shown on Figure 4.2.

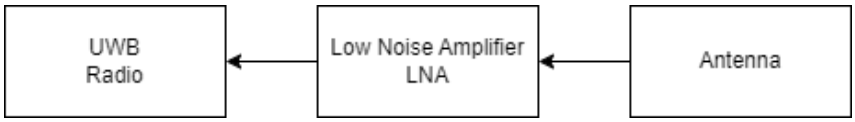

Figure 4.2: Proposed architecture for RX side UWB radio testing

4.3 Assessment of Existing Solutions

To determine the necessity for designing custom solutions, existing available solutions were analyzed.

4.3.1 Evaluation of existing UWB Modules

Several existing UWB evaluation kits were reviewed to assess their suitability for extended-range testing applications. Among them, the EVK1000 UWB Transceiver Evaluation Kit was identified as a promising candidate. However, the kit has been discontinued, with End-of-Life (EOL) status announced on March 24, 2021[19].

The recommended successors to this kit—DWM3001CDK and DWM3000EVB are equipped with integrated antennas. This limits system configurability, particularly in terms of amplifier integration or antenna replacement. Furthermore, both modules support only UWB channels 5 (6.5 GHz) and 9 (8 GHz), which restricts testing flexibility when compared to alternatives such as the DW1000, which supports six channels [20]–[22].

Other available evaluation platforms, such as those offered by SPARK Microsystems and Qorvo, were also considered. SPARK Microsystems provides multi-channel capability; however, the associated evaluation kits are priced significantly higher than other options, making them economically unviable for the scope of this thesis [23]. A similar issue was identified with Qorvo's newer development kits [24]. In addition, SPARK Microsystems' SDK and hardware documentation lack sufficient depth compared to competing manufacturers. Notably, the official website also exhibited poor performance during the research process, raising concerns about long-term accessibility of resources.

Due to the absence of suitable open and configurable evaluation kits, standalone UWB modules were investigated. The DWM1000 module was evaluated due to its ease of integration and Arduino software library support. However, it also includes an integrated antenna, limiting the possibility of signal chain modification [25]. A similar limitation applies to the DWM3000 module, the new revision of the DWM1000, which is also not suitable for use cases requiring flexible hardware architecture [26].

In conclusion, none of the mentioned existing commercial UWB development kits or modules met the specific configurability and channel range requirements necessary for long-range testing. This motivated the development of a custom UWB board tailored to the objectives of this work.

4.3.2 Amplifier Evaluation

Two commercially available amplifier modules sourced from Chinese suppliers were evaluated. Both claimed operation up to 6 GHz and were selected based on the requirement of achieving a minimum gain of 20 dB in the 3–5 GHz frequency range. The gain requirement was driven by the need to maximize transmission range. If necessary, the signal level could be reduced using external attenuators.

In general, it was observed that most low-cost amplifier modules are only rated up to 6 GHz. Above this frequency, available options become limited, and prices increase significantly. For this reason, lower UWB channels (1–4) in the 3–5 GHz range were preferred for cost-effective testing.

The first tested module, marketed as a "Signal Power Amplifier Board", is shown in Figure 4.3. The advertised specifications are listed in Table 4.1.

Table 4.1: Electrical and functional characteristics of 5M–6GHz RF amplifier module

Parameter	**Specification**
Operating Frequency	5–6000 MHz
Amplifier Gain	20 dB
Maximum Output Power	+21 dBm (100 mW) @ 1 dB compression point
Power Supply Voltage	5 VDC
Operating Current	85 mA (typical)
System Impedance	50 Ω
Dimensions	34 mm × 25 mm (1.33 × 0.98)

Figure 4.3: Signal Power Amplifier Board

Although the advertised gain appeared suitable (17–20 dB across 3–5 GHz), actual performance measurements using an R&S® ZND Vector Network Analyzer[27] in range of 3-5GHz, calibrated with the SDR-Kits SMA calibration kit[28], revealed a different result. The measured S_{21} parameter is shown in Figure 4.4.

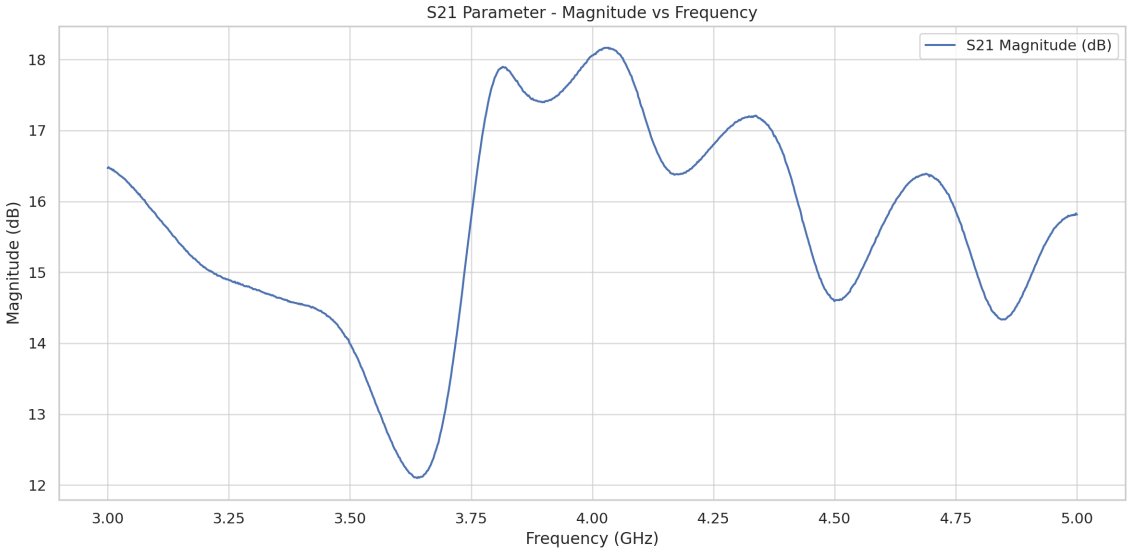

Figure 4.4: Measured S_{21} parameter (Gain)

The results show gain fluctuation across the frequency range. As UWB signals occupy a wide bandwidth, consistent gain across the entire spectrum is essential for preserving signal integrity.

A second amplifier module, marked NWDZ, was also tested (see Figure 4.5)[29]. Its advertised specifications are shown in Table 4.2.

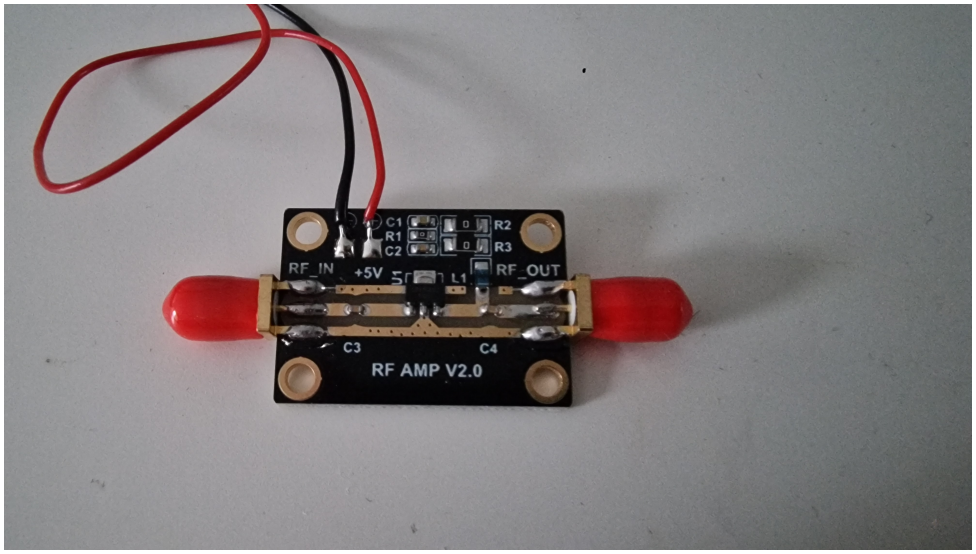

Figure 4.5: Amplifier NWDZ

Table 4.2: Electrical and functional characteristics of MMIC RF amplifier module (A49T)[29]

Parameter	**Specification**
Power Supply Voltage	+5 VDC (no dropping resistor required)
Operating Current	75 mA (typical)
Amplifier Gain	20 dB @ 2 GHz
Maximum Output Power	+20 dBm @ 1 dB compression point (2 GHz)
Input Signal Limit	Less than +10 dBm (distortion above this level)
Bandwidth	50 MHz – 6 GHz (gain varies by frequency)
Input/Output Impedance	50 Ω
Noise Figure	4.1 dB @ 1 GHz

Despite promising specifications, measured performance again deviated from the advertised values. The S_{21} parameter measurement is shown in Figure 4.6.

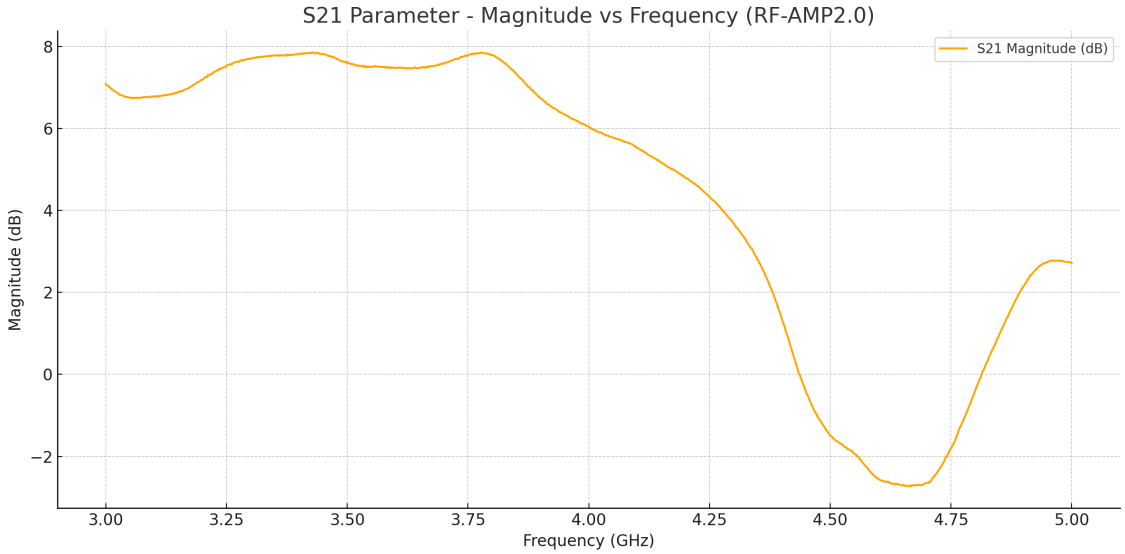

Figure 4.6: Measured S_{21} parameter of second amplifier

The testing configuration was identical to the previously described setup. Measurement results show gain variation. Notably, the amplifier exhibited negative gain values from 4.4 to 4.8 GHz, suggesting a defective or damaged module. So, these observations confirm that commercially available amplifier modules do not fulfill the required specifications. Therefore, a custom-designed amplifier is necessary.

4.3.3 Antenna Performance Assessment

The objective was to identify an omnidirectional antenna with an S11 parameter below $-10\,dB$ in wanted frequency range.

Multiple commercially available antennas were evaluated. Two antennas from the manufacturer Deepace were selected for further study, shown in Figure 4.7 and Figure 4.8. Manufacturer specifications are listed in Table 4.3.

Table 4.3: Specifications of DEEPACE Wideband Omnidirectional Antennas[30][31]

Parameter	**DEEPACE v1**	**DEEPACE v2**
Frequency Range	3.1–9 GHz	2.8–11 GHz
Polarization Mode	Linear	Linear
Rated Gain	2 dBi	3.8 dBi
Return Loss	10 dB	10 dB
Power Capacity	5 W	5 W
Connector Type	SMA-K	SMA-K
Mechanical Size	35 mm × 22 mm (excluding connector)	30 mm × 42 mm (excluding connector)
Directionality	Omnidirectional	Omnidirectional

Figure 4.7: Deepace UWB-1 Antenna

Figure 4.8: Deepace UWB-2 Antenna

No radiation pattern data was provided by the manufacturer, apart from the stated omnidirectional nature and gain values (2 dBi and 3.8 dBi, respectively).

S11 measurements were carried out using an R&S® ZND Vector Network Analyzer[27] in the 3–5 GHz range. The setup was calibrated using the SDR-Kits SMA calibration kit[28]. Measurement bandwidth was 10 kHz and power level was set to 3 dBm. (Note: Although the measurement image indicates that calibration was off, it was in fact active during measurement.)

The measured results are shown in Figures 4.9 and 4.10.

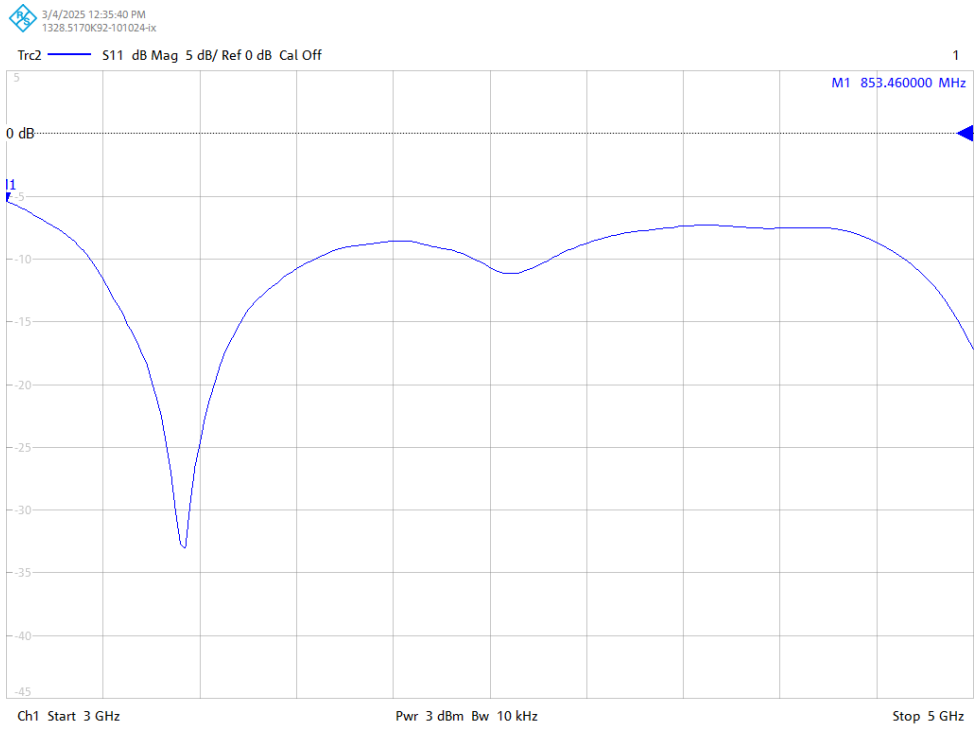

Figure 4.9: Measured S11 parameter for Deepace UWB-1

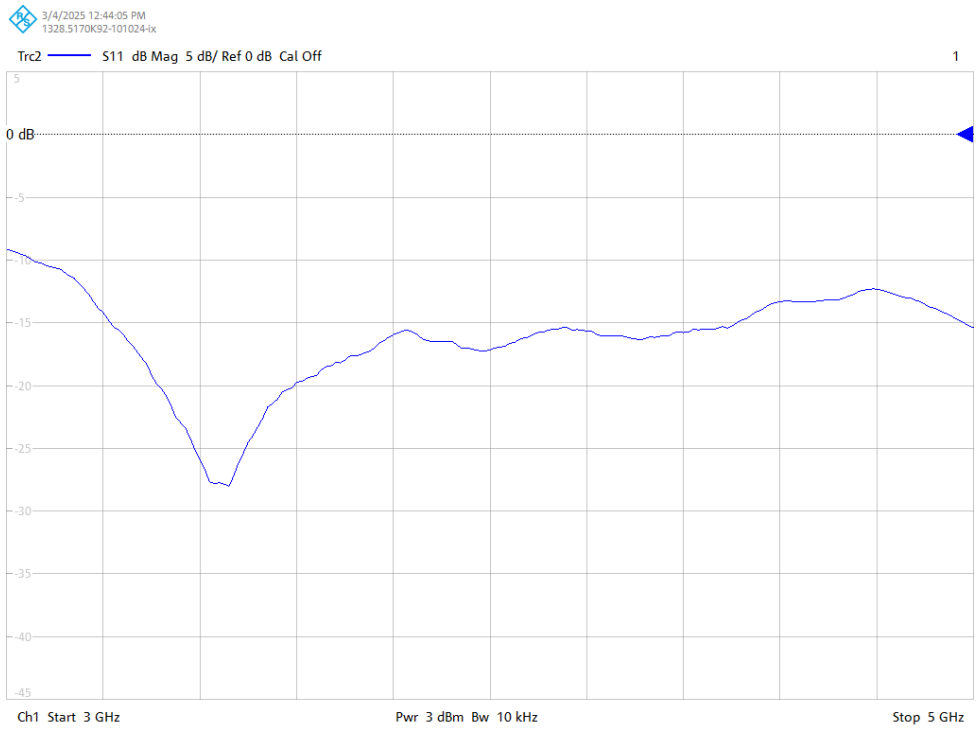

Figure 4.10: Measured S11 parameter for Deepace UWB-2

As shown in Figure 4.9, the UWB-1 antenna is matched between 3.15–3.6 GHz. Outside this range, the return loss exceeds $-10\,dB$, contradicting the given specifications for the antenna and making the use of this antenna non-ideal.

In contrast, the UWB-2 antenna (Figure 4.10) shows it is matched better the in working frequency range. However, the S11 values fluctuate significantly, with a sharp dip to $-27\,dB$ at 3.45 GHz. An antenna offering more uniform S11 behavior across the 3–5GHz band is desirable.

In conclusion, neither antenna provides a consistant S11 response across the desired bandwidth. The antennae could be used but they would be non-ideal. A more broadband and impedance-stable antenna design is required. Additionally, relying on commercially available antennas introduces a dependency on the manufacturer, which may hinder reproducibility if the antenna design changes or becomes unavailable.

4.4 Justification for Custom Design

Commercially available UWB modules, such as the DWM1000 and DWM3000, are limited by integrated antennas and restricted channel support. Additionally, other platforms either lacked necessary documentation, had high cost, or showed limited hardware configurability.

Amplifier modules sourced from low-cost suppliers were tested, but both exhibited significant gain variation across the 3–5 GHz band. This is unacceptable for goal of this thesis to test the range of the UWB radio. Despite promising specifications, none of the tested amplifiers performed as expected.

Similarly, antenna evaluations revealed that neither tested model maintained consistent S11 values across the required frequency band. UWB-1 failed to meet basic bandwidth specifications, and while UWB-2 provided broader coverage, its return loss varied significantly. Given these limitations—and to ensure full control over design, performance, and supply chain—a custom antenna was developed.

Due to the limitations of available modules, amplifiers, and antennas, a custom deisgned system is necessary to be developed this allows the system to be as known as possible.

4.5 Design and Development of Custom Components

This section provides a detailed overview of the developed components for UWB extended-range communication. The electronics design was in Altium (version 2025.04) and for programming STM32CubeIDE (version 1.14.0) was used.

4.5.1 Custom UWB Board

Several UWB transceiver chips were evaluated to determine the most suitable option for a custom design.

The considered UWB chips include the DW1000, DW3000, QM33120W, SR1010, and SR1020. Some chips, such as NXP's SR040, were excluded due to lack of availability through public electronic distributors. Table 4.4 presents a comparison of the transceivers, highlighting specifications such as supported channels, data rates, and pricing. In addition, availability of development resources (SDKs, libraries, documentation) is also taken into concideration.

Table 4.4: Comparison of UWB Transceivers (IEEE Channels and Specs)[22] [32] [24] [33] [34]

Transceiver	**Supported Channels (IEEE)**	**Supported Data Rates**	**Price (EUR)**
DW1000	Channels 1–5, 7	110 kbps, 850 kbps, 6.8 Mbps	€10.5
DW3000	Channels 5, 9	850 kbps, 6.8 Mbps	N/A (Not publicly listed)
QM33120W	Channels 5, 9	850 kbps, 6.8 Mbps	€12.1
SR1010	Channels 1–4[1]	1 kbps to 10 Mbps[2]	€6.60
SR1020	Channels 5–11[1]	1 kbps to 10 Mbps[2]	€6.60

[1] Estimated channel mappings based on IEEE 802.15.4 frequency allocations and datasheet frequency ranges[35].
[2] Data rate derived from fixed 20.48 Mbps symbol rate and modem features including OOK modulation, differential encoding, and punctured FEC (rates 1.0, 1.33, 1.66, 2.0); effective data rate depends on packet format and FEC.

From the comparison, two transceivers stand out: the DW1000 and the SR1020. Both offer wide channel support and relatively low cost. Among these, the DW1000 was selected for the custom UWB board due to its mature development ecosystem. It has a well-documented API and STM32 examples, online resources and community support.

The DW1000 communicates via SPI. Therefore, the selected microcontroller must support SPI (at 3.3 V) and include a USB interface to enable communication with a computer. Since STM32-based examples for the DW1000 exist a STM32 MCU (STM32F103C8T6TR) was chosen.

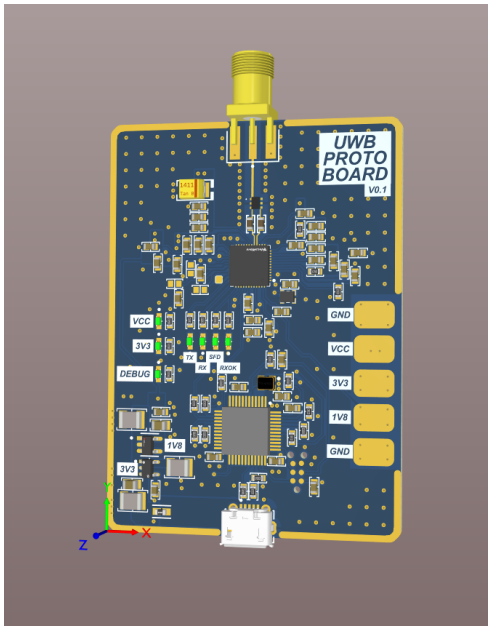

Figure 4.11: Developed UWB board in Altium

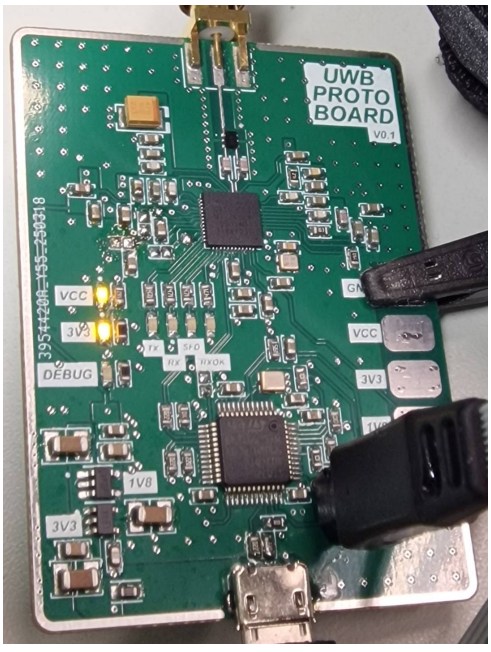

Figure 4.12: Developed UWB board in real life

Figures 4.11 and 4.12 show the developed UWB board as designed in Altium and its physically assembled version, respectively. The board underwent two iterations (versions 0.0 and 0.1). Between these iterations, the primary modifications involved changes to the PCB stack-up, minor bug fixes, and improvements to board configurability. The overall system architecture of the developed board is presented in Figure 4.13.

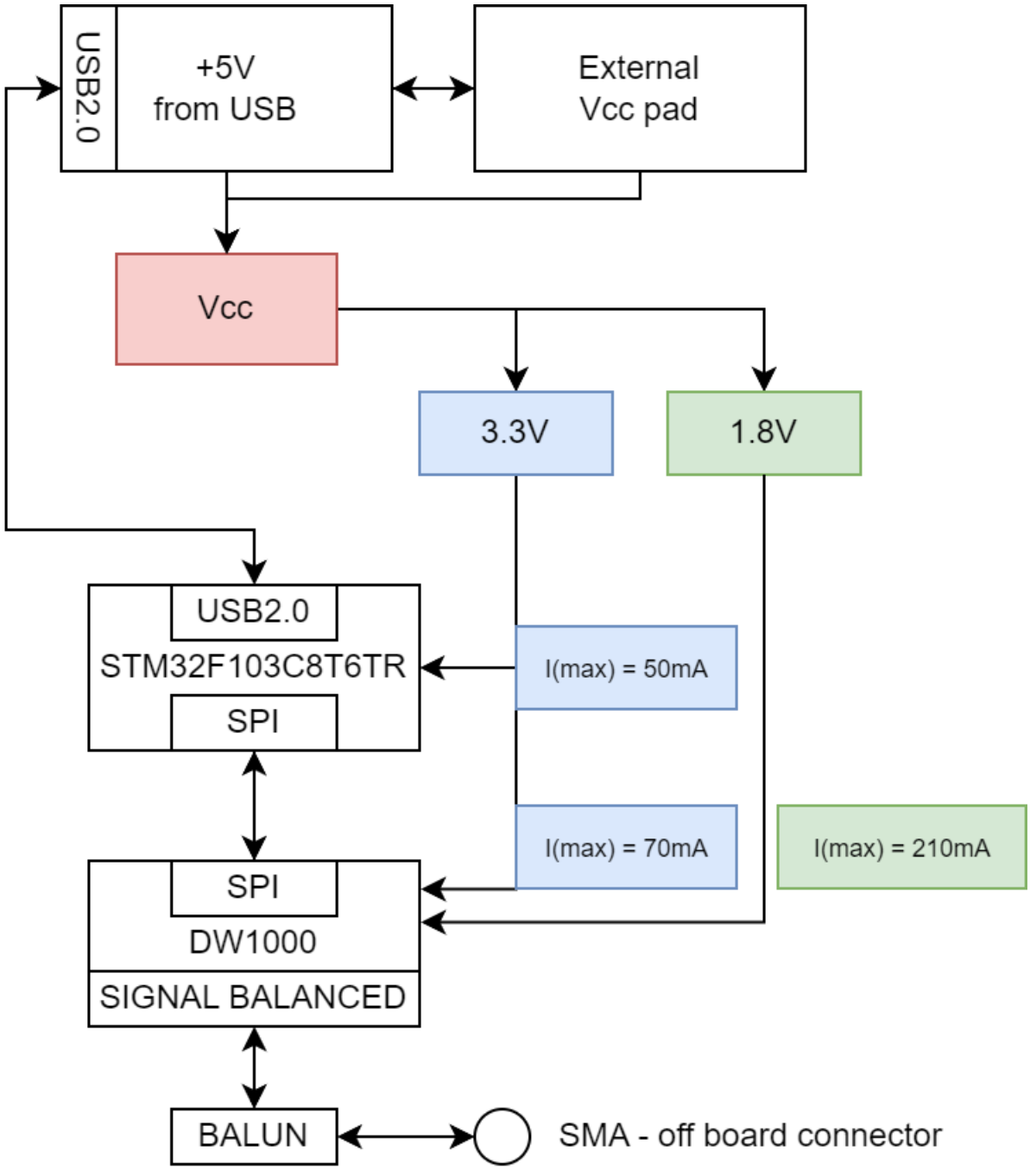

Figure 4.13: UWB board top-level architecture showing power distribution and interfaces

JLCPCB was selected as the manufacturer based on previous positive experiences, competitive pricing, and suitable manufacturing capabilities. A four-layer PCB (stack-up JLC04161H-7628) was chosen. The proximity of the ground plane (top most internal layer) to the signal layer (top layer) allowed narrower traces, facilitating a 50 Ω characteristic impedance. A two-layer

design would have required significantly wider traces. The manufacturer's impedance calculator determined a 50 Ω transmission line trace width of 0.349 mm.

Voltage regulators TLV75518PDBVR and MIC5219-3.3YM5-TR were selected for generating the 1.8 V and 3.3 V rails, based on their current capabilities and low-noise characteristics.

On the USB interface, a ferrite bead was included to reduce high-frequency noise. Bulk capacitors with relatively high capacitance values were added for improved voltage stability. Series termination resistors (22 Ω) were placed on the USB data lines for proper termination, and a 1.5 kΩ pull-up resistor was included on the USB D+ line to comply with the USB 2.0 specification.

For programming and debugging, a TAG connector compatible with the STLINK-V3 and the TC2030-CTX-NL-STDC14 cable was integrated. Debugging LEDs were also included to visually verify power status; these LEDs could be omitted in future revisions to reduce power consumption.

Communication between the STM32 microcontroller and the DW1000 transceiver was implemented via SPI, with 22 Ω series termination resistors to maintain signal integrity. The chip-select (CS) line included a 10 kΩ pull-up resistor.

At the DW1000 RF output, a balanced transmission line with a target impedance of 100 Ω per trace was implemented. The manufacturer's impedance calculator yielded a required trace width of 0.272 mm with the spacing of 0.407 mm. However, due to physical constraints imposed by the DW1000 package, the practical trace width was reduced to 0.175 mm, resulting in an impedance mismatch. The balanced differential signal was converted to a 50 Ω single-ended output using a BAL-UWB-01E3 balun. The resulting single-ended signal was output via an SMA connector.

Four additional LEDs were included for debugging DW1000 operations, indicating transmission (TX), reception (RX), start frame delimiter (SFD) detection, and successful packet reception (RxOK). Additionally, a dedicated pad was included to optionally enable or disable an external amplifier if deemed necessary.

The board was assembled manually by applying solder paste using a stencil, followed by component placement and solder reflow using a reflow oven.

Complete design documentation, including schematic diagrams, PCB layouts, and the bill of materials, are provided in the appendices (*Appendix – I. UWB Board Schematic, Appendix – II. UWB Board PCB Layout, Appendix – III. UWB Board Bill of Materials*).

4.5.2 Custom Amplifier

Amplifier Requirements

The design requirements are summarized in Table 4.5.

Table 4.5: Amplifier Design Requirements

Parameter	**Specification**
Max Voltage	5 V
Gain	As high as possible
Frequency Range	3 GHz – 5 GHz
Input/Output Impedance	50 Ω

A suitable component for this purpose is the Renesas F1485 amplifier, which meets all design requirements.

Manufacturer Specifications

Table 4.6: Renesas F1485 RF Amplifier Specifications [36]

Parameter	**Value**
Frequency Range	2.3 GHz – 5.0 GHz
Gain	36.5 dB @ 3.6 GHz
Noise Figure (NF)	3.8 dB @ 3.6 GHz
Output Power at 1 dB Compression (OP1dB)	27 dBm @ 3.6 GHz

Gain variation across frequency bands is provided in Table 4.7.

Table 4.7: Gain Variation across Frequency Bands [36]

Frequency Range (MHz)	**Gain Variation (dB)**
2300 – 2700	0.25
3300 – 3800	0.10
3800 – 4200	0.40
4400 – 5000	2.80

From Table 4.7, gain flatness increases at higher frequencies. The goal is to keep this value as low as possible to ensure linear gain.

Custom Amplifier Design

A custom RF amplifier was designed based on the Renesas F1485 amplifier, suitable for UWB within the frequency range of 3–5 GHz. Initial component values were selected according to guidelines provided by Renesas in the F1485 Wideband Application Note.

The PCB layout was implemented in Altium Designer. Manufacturing was done by JLCPCB. It was selected due to cost-effectiveness and previous experiences with their production. To know transmission line impedances a specific PCB stack-up "JLC04161H-3313" was used. According to the manufacturer's impedance calculator, a trace width of 0.1565 mm was determined to achieve

a characteristic impedance of 50 Ω. This relatively narrow trace width was also advantageous due to the compact dimensions of the amplifier package.

SMA panel edge male connectors were used at the edges of PCB for connecting the signal path. Although a SMA female connector is shown in the initial Altium rendering (Figure 4.14), in the real life version(Figure 4.15) male connectors were chosen due to their availability. SMA female-to-female connectors were used to tie things togheter.

Component packages of size 0402 were selected for passives to minimize parasitics. Additionally, multiple zero-ohm resistors and Do-Not-Populate placeholders for capacitors were included in the design to allow for flexibility during testing.

Through iterative tuning, it was determined that inserting a 2 pF capacitor in series and a parallel to ground 33 pF capacitor at the amplifier input provided the best results. S11 was sacreficed for the gain to be as uniform as possible. This could be futher improve upon in the future.

In the prototype configuration, the amplifier biasing pins V_{bias}, V_{ref}, and STBYb were interconnected.

The schematic diagram, detailed PCB layout, and complete BOM for the amplifier board are provided in the appendix for reference:

- Appendix – IV. Amplifier Schematic
- Appendix – V. Amplifier PCB Layout
- Appendix – VI. Amplifier Bill of Materials

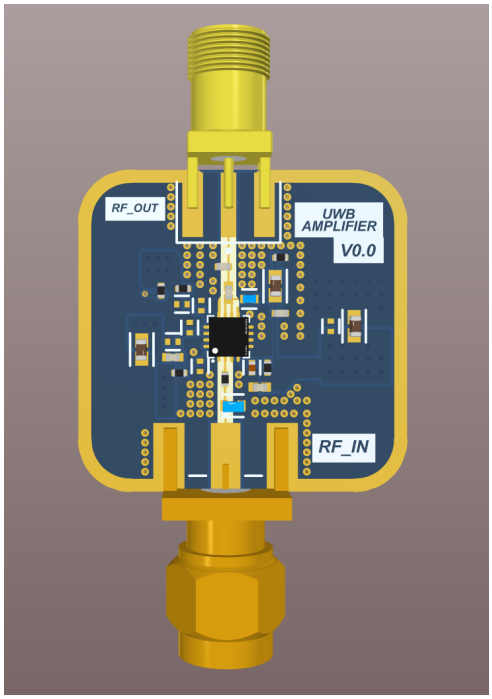

Figure 4.14: Custom amplifier design in Altium

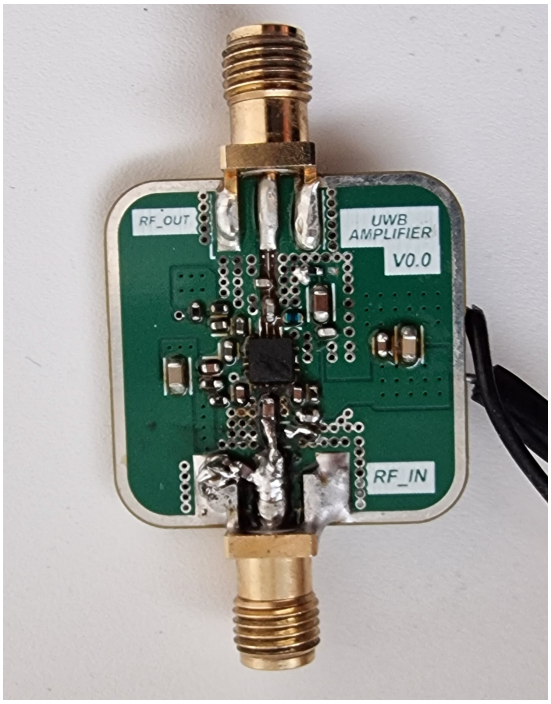

Figure 4.15: Developed UWB amplifier in real life

This design was ordered and tested. The measured current consumption at 5 V supply was 0.108 A.

The amplifier Scatter parameters were measured using an R&S® ZND Vector Network Analyzer in the 3–5 GHz range. Calibration was performed with the SDR-Kits SMA calibration kit. Measurement bandwidth was 10 kHz and the signal power was set to –14.32 dBm.

S-Parameter Results

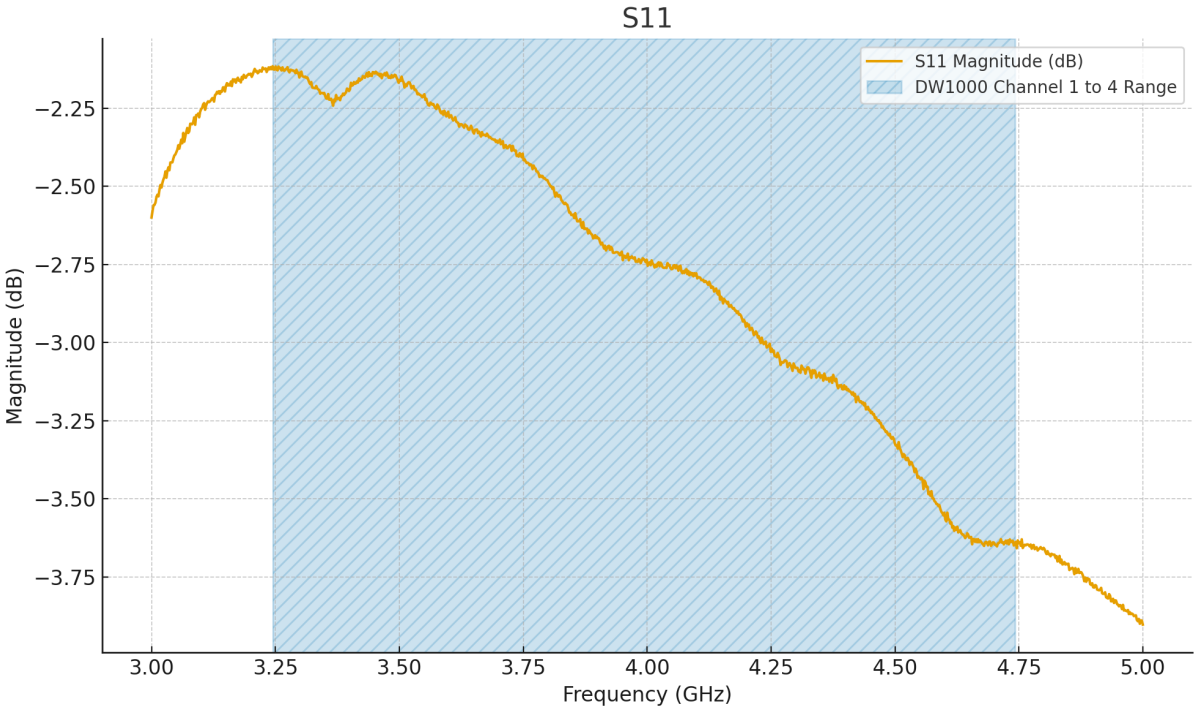

Figure 4.16: S_{11} magnitude response at amplifier input

S_{11} measured –2.76 dB ± 0.48 dB. Ideally, values below –10 dB are preferred, but in this design, matching was sacrificed to prioritize gain linearity. Matching was tuned using a 2 pF series and 33 pF parallel capacitor.

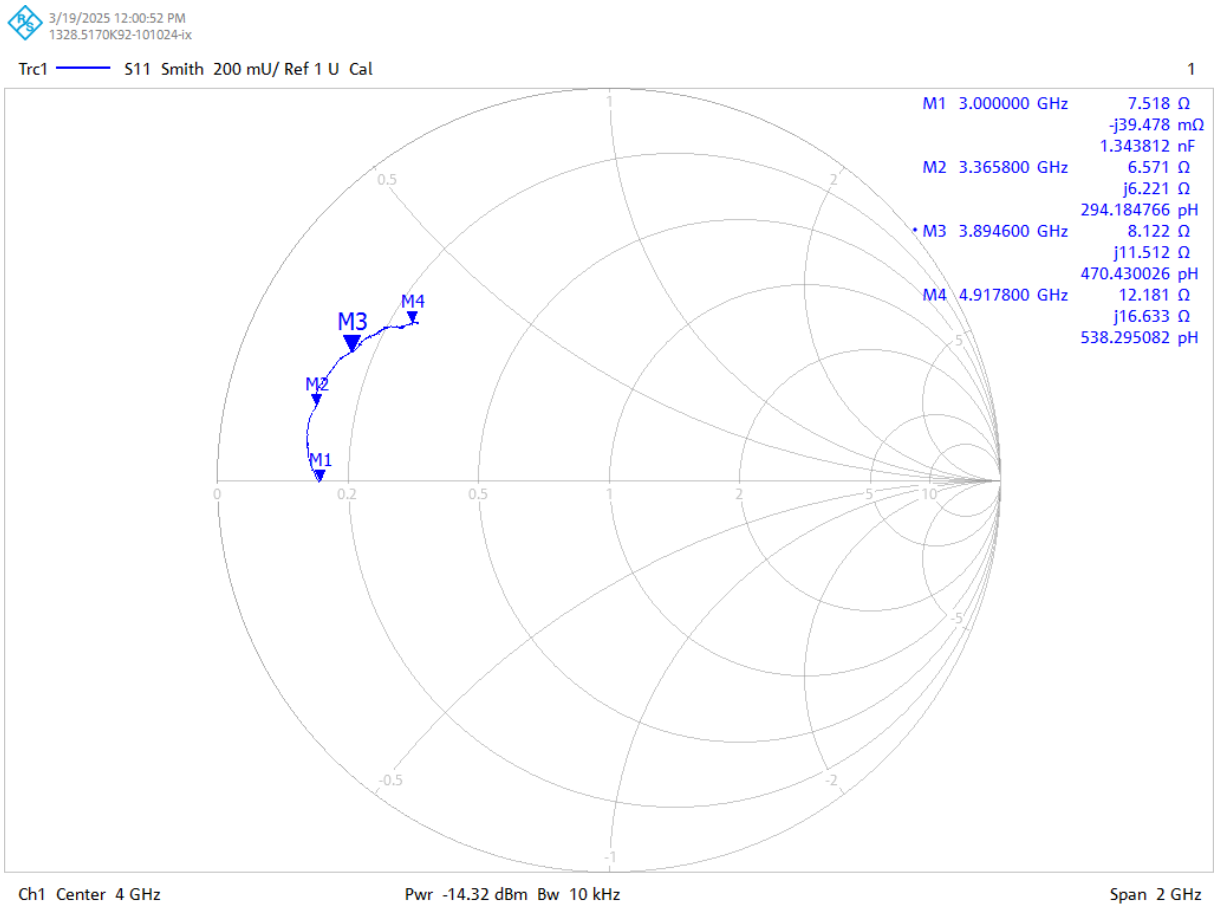

Figure 4.17: S_{11} Smith chart—inductive input

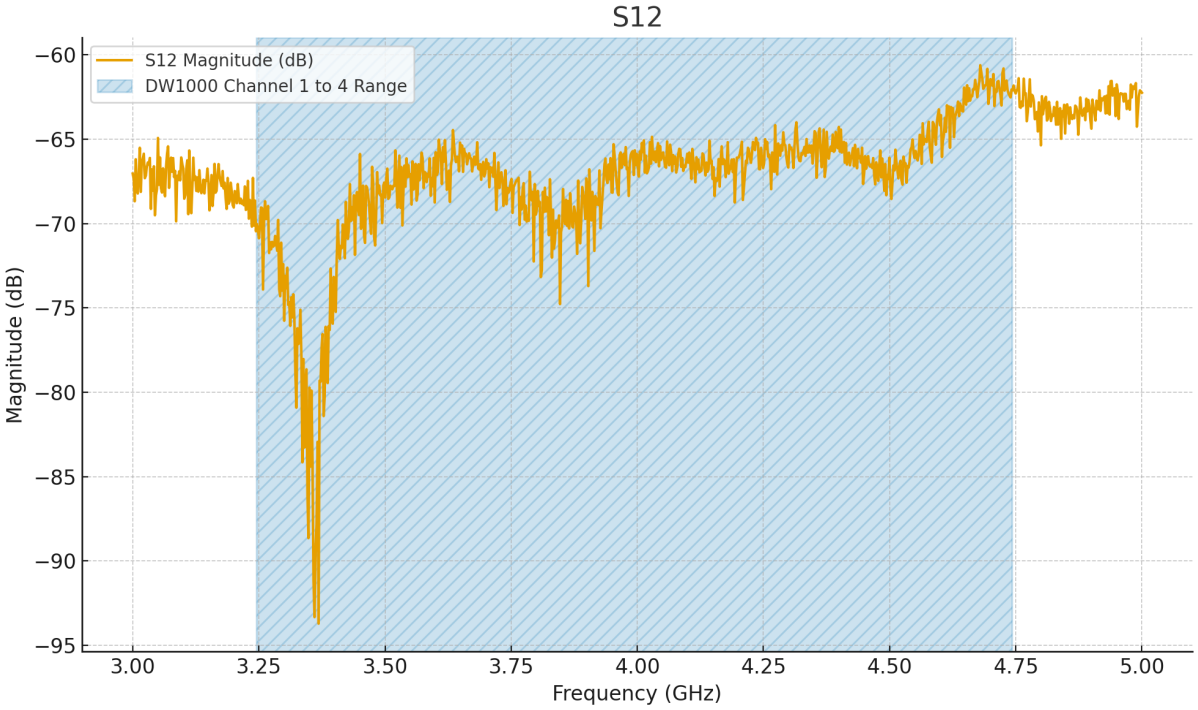

Figure 4.18: S_{12} magnitude response—reverse isolation

Reverse isolation S_{12} averaged –67.61 dB ± 4.10 dB. A spike to –94 dB at 3.375 GHz was observed, but it does not play a role in this use case.

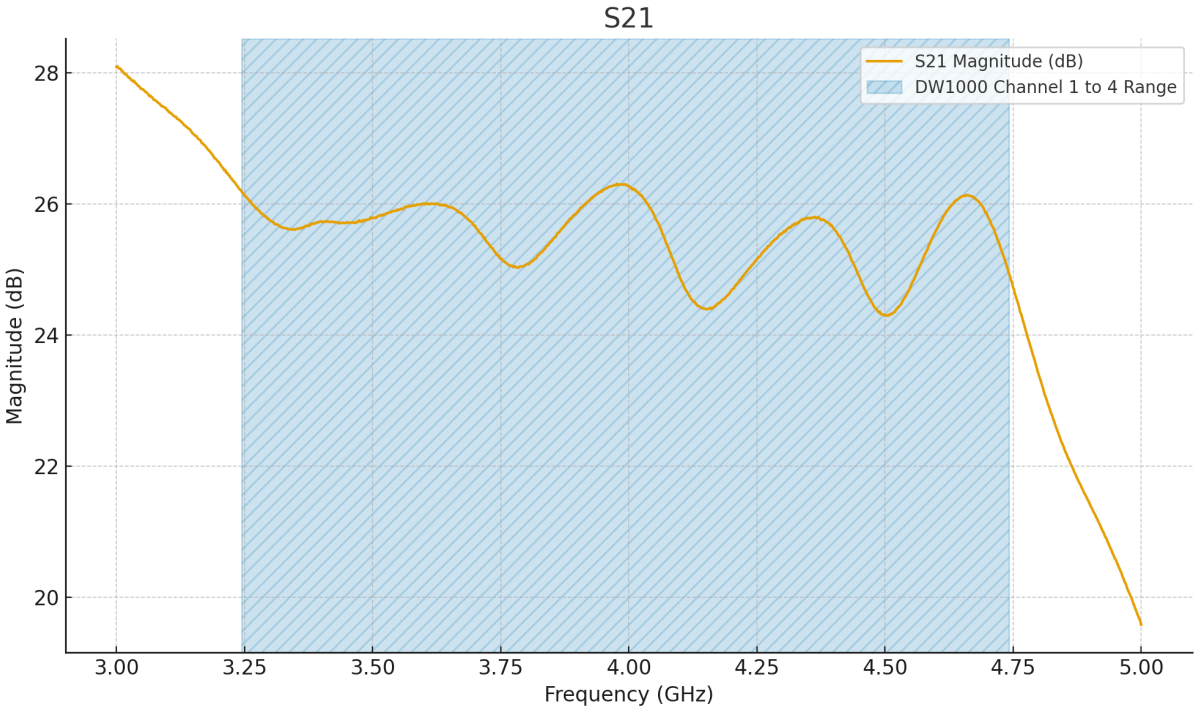

Figure 4.19: S_{21} magnitude response—forward gain

S_{21}, representing forward gain, averaged 25.50 dB ± 0.52 dB. This indicates good gain flatness, aligning with the expected range from the manufacturer's specifications.

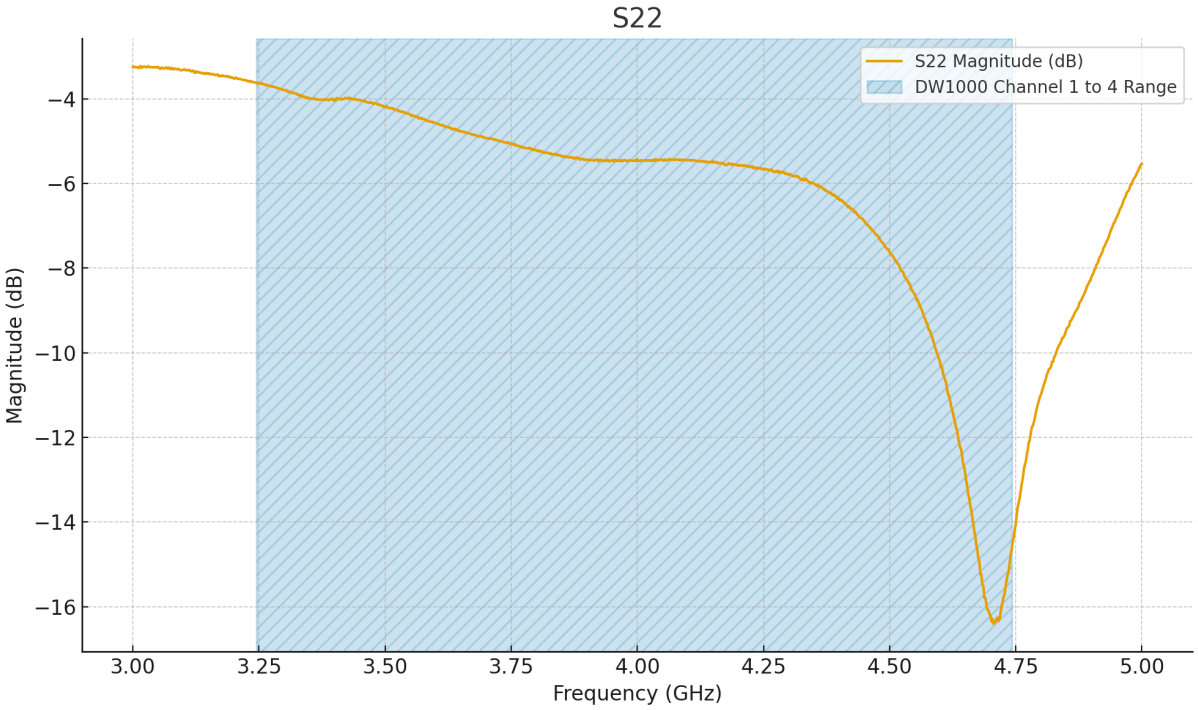

Figure 4.20: S_{22} magnitude response at output

Output reflection S_{22} averaged –6.22 dB ± 2.84 dB. A sharp dip is caused by suboptimal LC network selection.

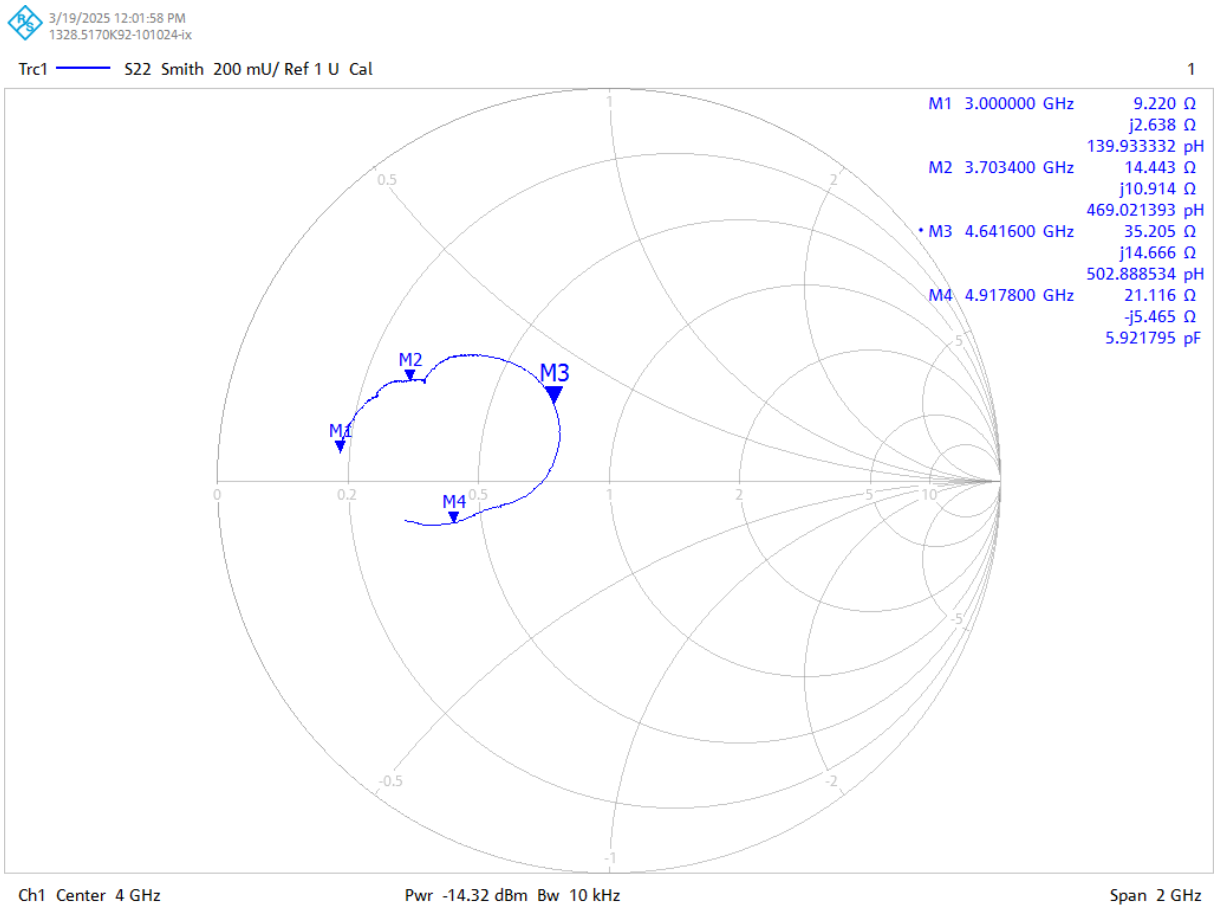

Figure 4.21: S_{22} Smith chart—inductive output

The S_{22} Smith chart confirms the output is too inductive. Future improvements will focus on improving output matching through better inductor and capacitor selection.

4.5.3 Custom Antenna Design

The custom antenna was based on the super wideband pentagonal structure proposed in *"Split–ring resonator loaded pentagon antenna for super wide band communications"* [37]. However, the full set of properties discussed in the original paper was not required for this application. The design was therefore simplified while retaining the core geometry.

Antenna Design and Simulation

Design and simulation were conducted using COMSOL Multiphysics (v5.2) with the RF Module. The design target was operation in the 3–5 GHz range.

The initial geometry values were derived from a quarter-wavelength resonator corresponding to the lowest frequency of interest:

$$\lambda = \frac{c}{f} = \frac{3 \times 10^8\ m/s}{3 \times 10^9\ Hz} = 100\ mm, \quad \frac{\lambda}{4} = 25\ mm$$

Assuming an effective resonator height $h = 25\ mm$, the side length S of a regular pentagon was calculated as follows:

$$S = \frac{2h}{\sqrt{5 + 2\sqrt{5}}} = \frac{2 \times 25}{\sqrt{5 + 2\sqrt{5}}} \approx \frac{50}{3.078} \approx 16.24\ mm$$

This value was used as a lower bound in geometry optimization.

Substrate and Material Properties:
The antenna was simulated on a PTFE-based substrate with the following parameters:

- Dielectric constant: $\varepsilon_r = 2.94$
- Substrate thickness: 0.76 mm

Material specifications were obtained from the PCB manufacturer (JLCPCB).

Optimization Procedure:
A two-stage hybrid optimization approach was applied:

1. *Global search:* Monte Carlo sampling identified promising regions in the parameter space.
2. *Local refinement:* Nelder–Mead algorithm to futher minimize the S_{11} parameter.

The optimization objective was to minimize the sum of squared deviations from ideal S_{11} behavior over the frequency range 3–5 GHz, sampled at 0.1 GHz intervals:

$$ObjectiveFunction: \quad \min \sum_{f=3\ GHz}^{5\ GHz} (20 - |S_{11}(f)|)^2$$

The parameters optimized to achieve the lowest S_{11} values were the pentagon side length (S), ground slot length (L_{slot}), ground plane length (L_g), and feedline length (L_f).

The optimized antenna geometry is illustrated in Figures 4.22 and 4.23. The values are shown in Table 4.8.

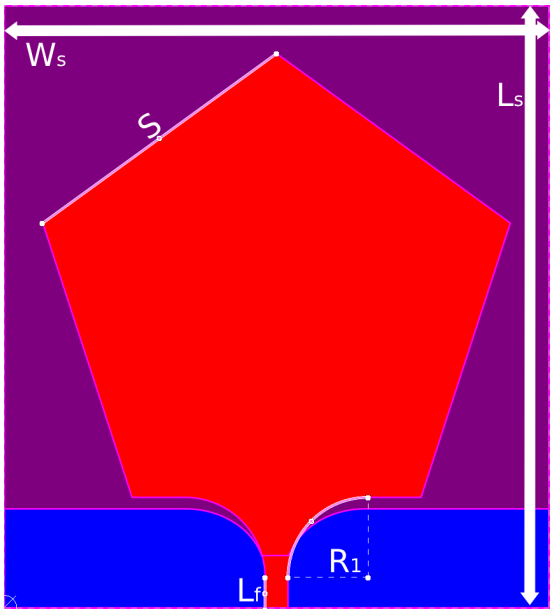

Figure 4.22: Optimized antenna geometry – top view

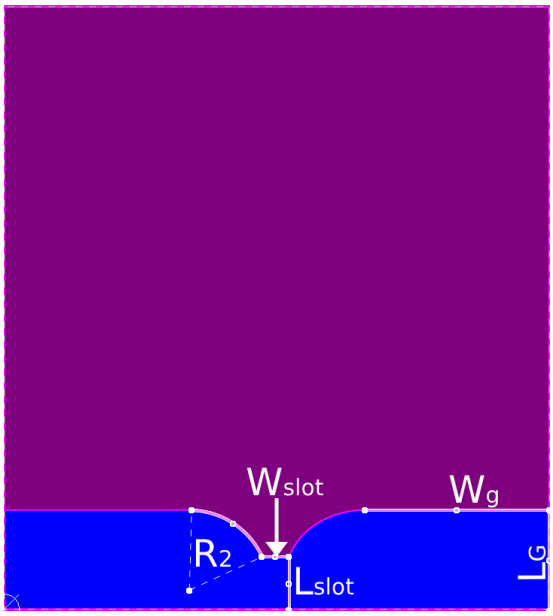

Figure 4.23: Optimized antenna geometry – bottom view

Table 4.8: Optimized antenna geometry values

Parameter	Value (mm)
Pentagon side length (S)	26.5
Ground slot length (L_{slot})	6.0366
Ground plane length (L_g)	9.2879
Feedline length (L_f)	10.349
Substrate width (W_s)	50
Substrate length (L_s)	45
Slot radius (R_1)	7.349
Slot width (W_{slot})	2.5
Ground width (W_g)	17.9
Ground slot radius (R_2)	6.2879

This produced the following radiation patterns that are shown in figures 4.24,4.25,4.26 and 4.27.

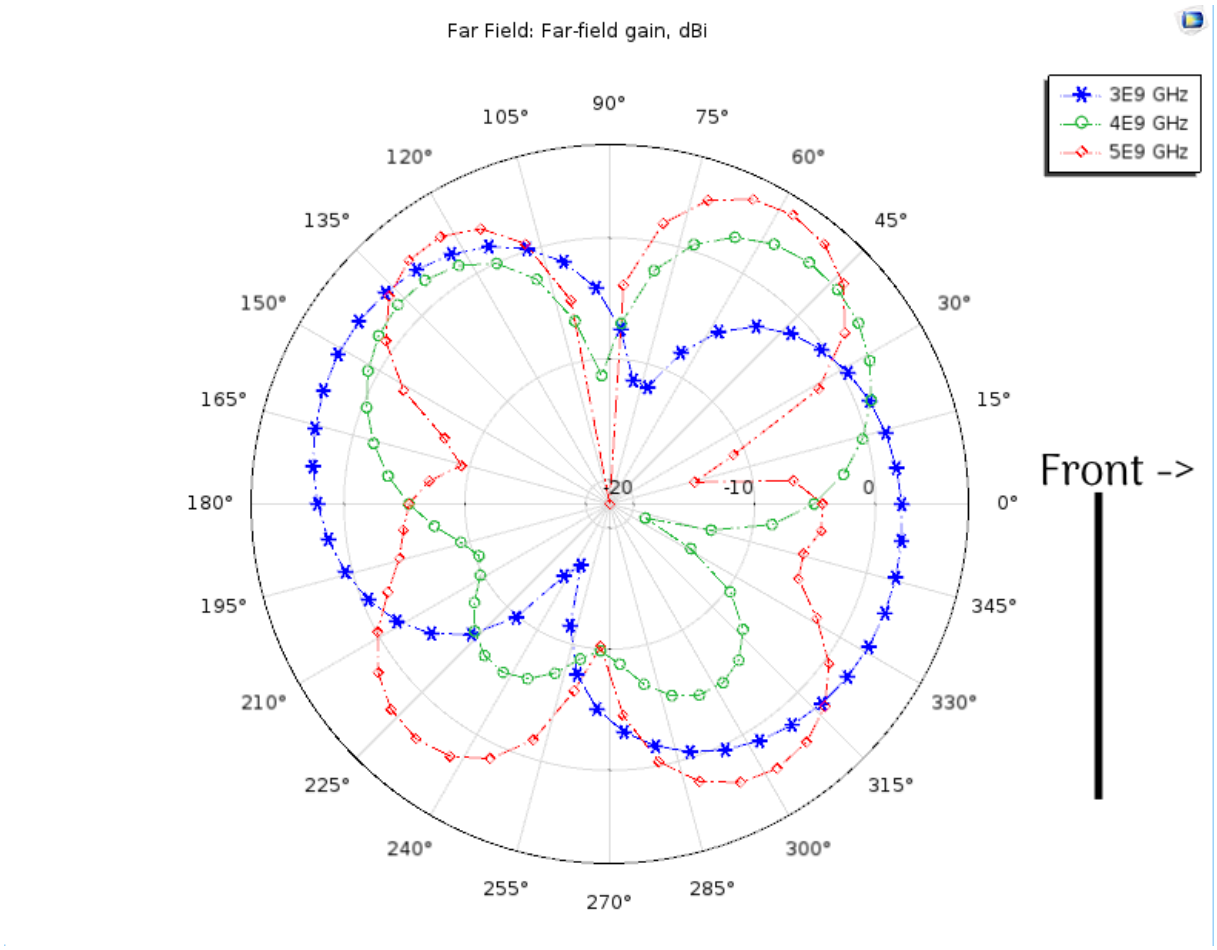

Figure 4.24: Simulated radiation pattern – top view

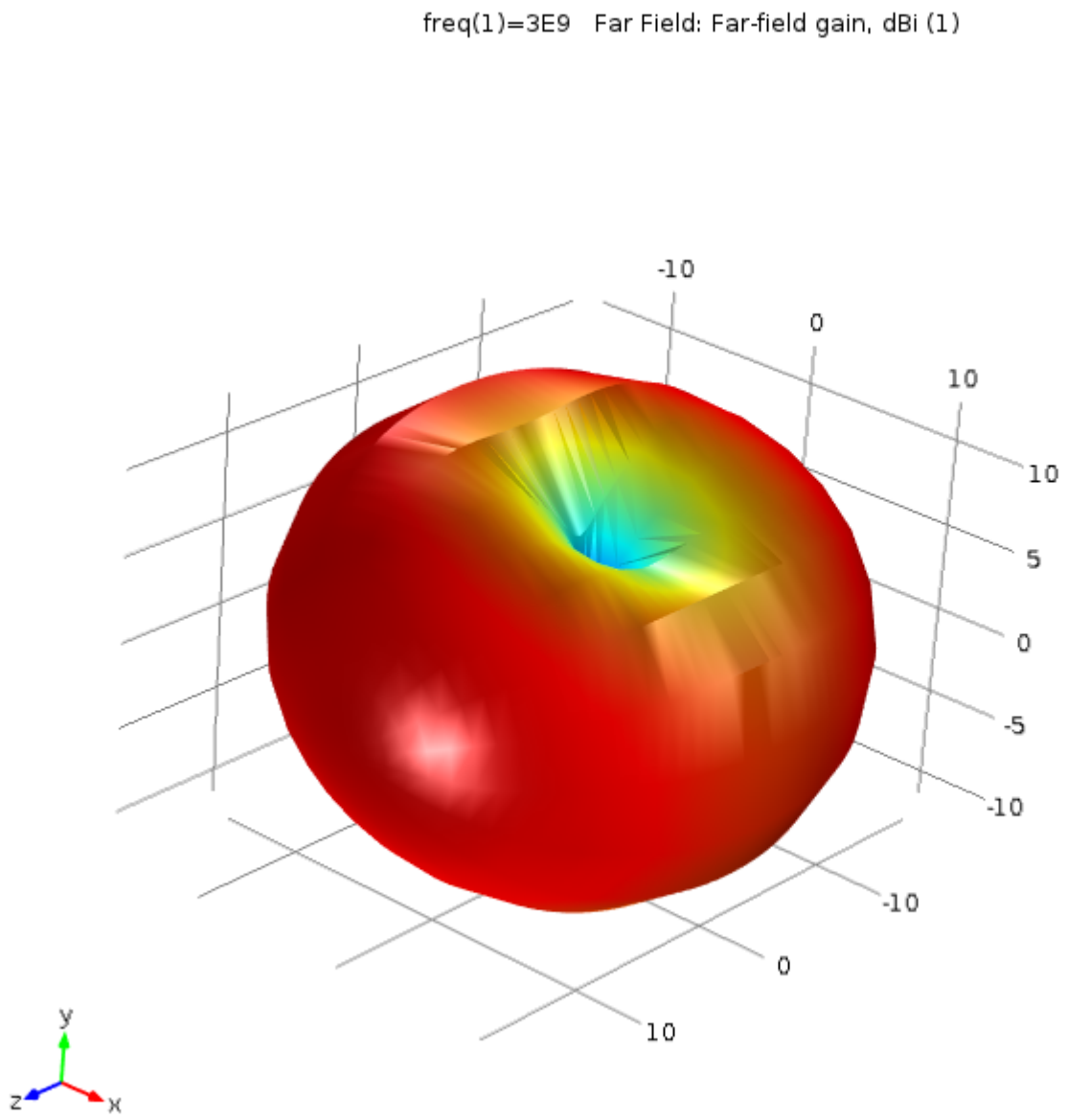

Figure 4.25: Simulated radiation pattern – Far field at @ 3 GHz

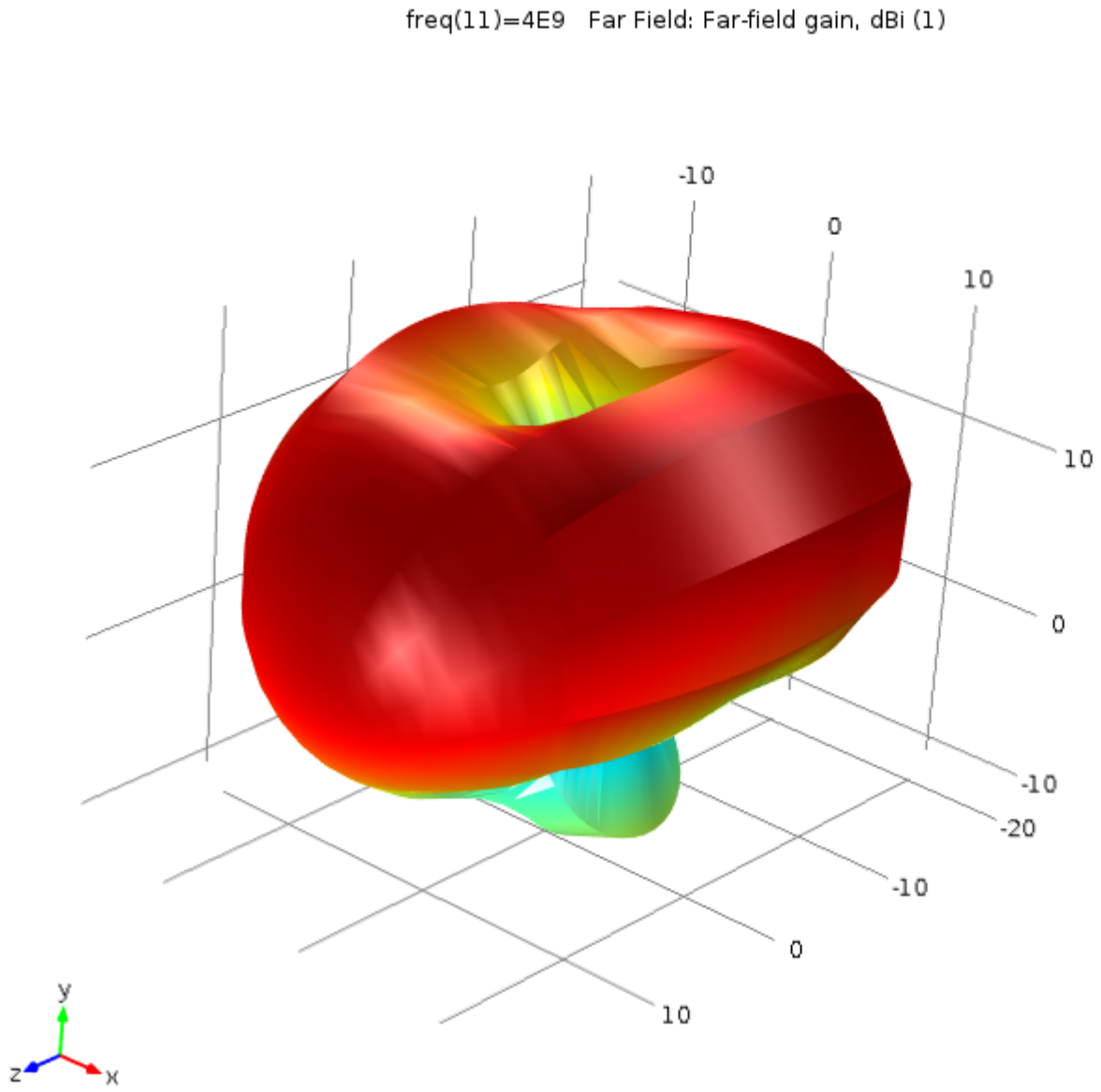

Figure 4.26: Simulated radiation pattern – Far field at @ 4 GHz

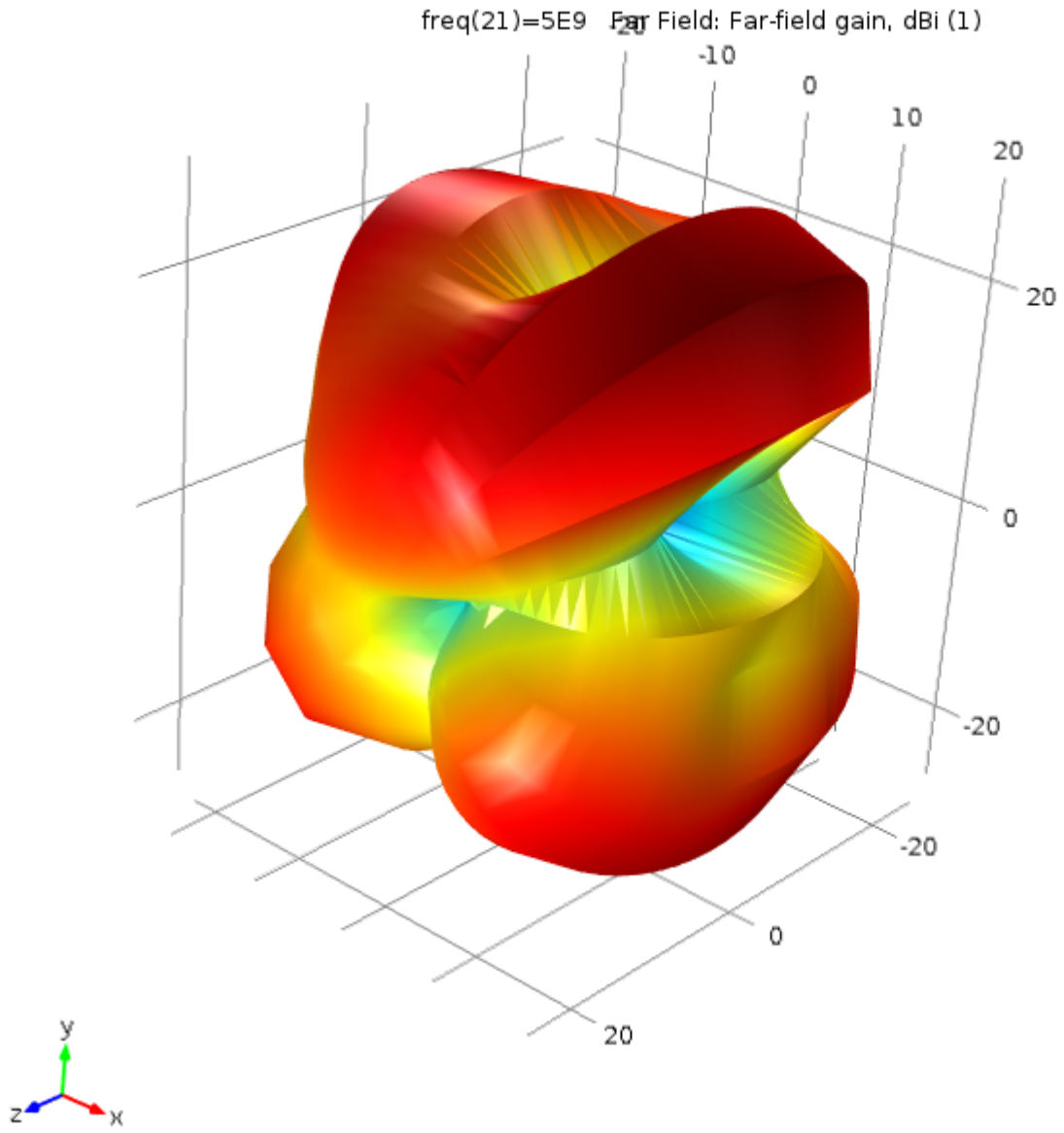

Figure 4.27: Simulated radiation pattern – Far field at @ 5 GHz

Manufacturing

After the antenna was simulated and optimzed the antenna was manufactured. Real-world implementation of the antenna is shown in Figure 4.28 and Figure 4.29.

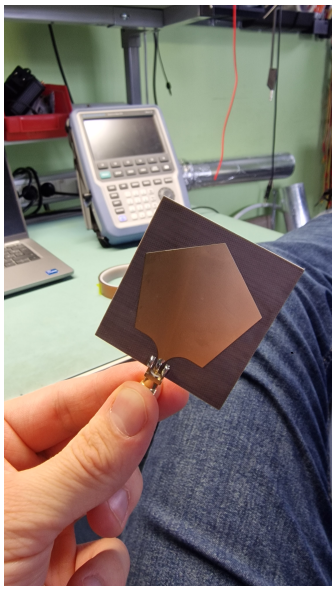

Figure 4.28: Manufactured antenna front view

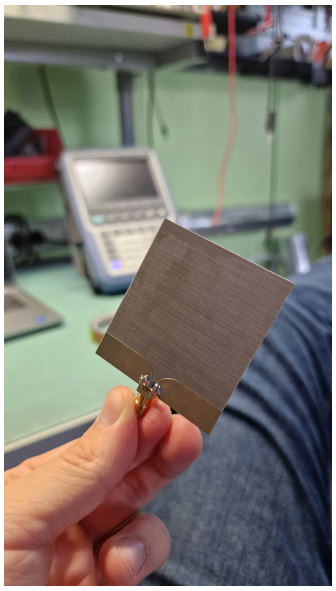

Figure 4.29: Manufactured antenna back view

The measured and simulated S_{11} parameters are compared in Figure 4.30. The UWB channels highest and lowest frequencies are highlighted. Measurements were conducted using an R&S® ZND Vector Network Analyzer [27], calibrated with an SDR-Kits SMA calibration kit [28].

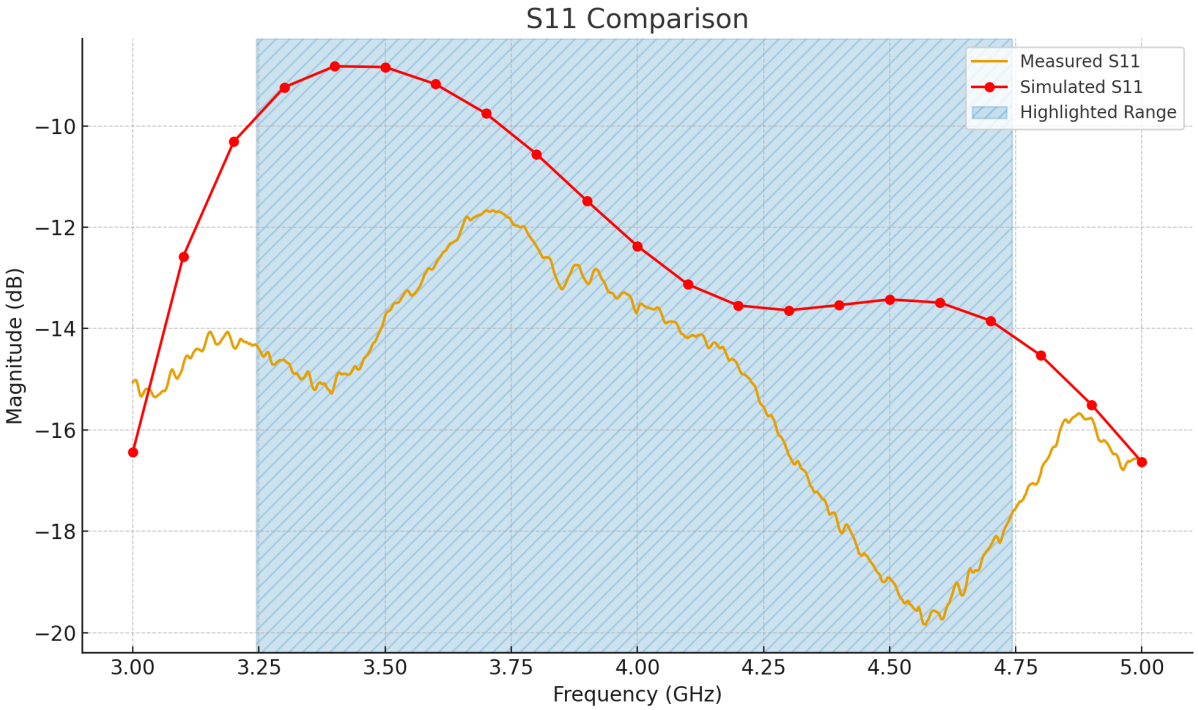

Figure 4.30: Simulated vs measured S_{11} parameters

Performance Summary:

- Simulated S_{11}: -12.42 dB ± 2.38 dB

- Measured S_{11}: -15.23 dB ± 2.18 dB

While the measured and simulated results generally align in trend, a noticeable difference of several dB is present. This discrepancy is likely due to imperfections in the SMA connector region, which were not included in the simulation. Nonetheless, the overall correspondence confirms the prototype was manufactured in closely to the simulated one.

4.6 Summary

Evaluation of commercially available UWB modules, amplifiers, and antennas revealed limitations in configurability, frequency coverage, linearity, and impedance matching. These constraints made them unsuitable for long-range UWB experimentation.

To overcome these issues, custom components were designed, including a UWB transceiver board based on the DW1000, a high-gain RF amplifier based on Renesas F1485, and pentagonal antenna optimized for performance in the 3–5 GHz range.

The custom design approach ensures full control over signal path and hardware flexibility.

5 Testing

To evaluate the practical range capabilities of the UWB system under realistic outdoor conditions tests were performed. All tests were cordinated with the Estonian frequency allocation authority (Consumer Protection and Technical Regulatory Authority). A special frequency permit (SLM-25-0142) was given out for the testing.

5.1 Hardware setup

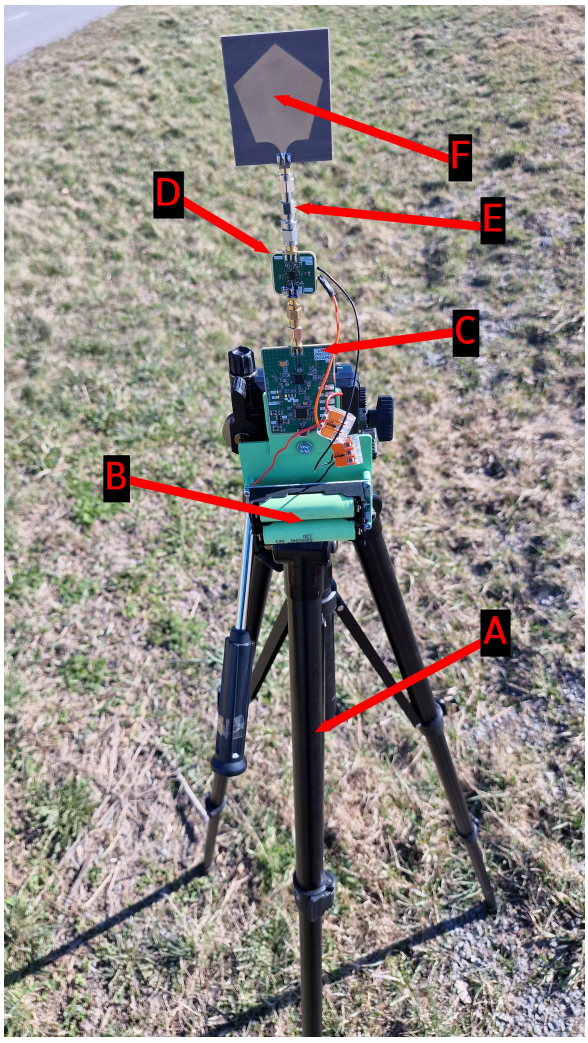

Figure 5.1: TX testing setup

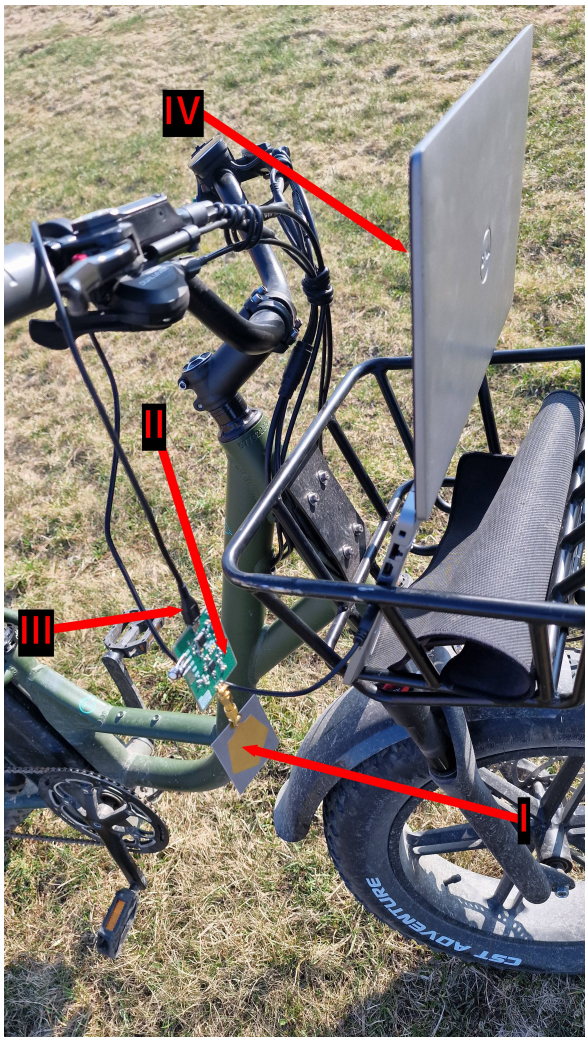

Figure 5.2: RX testing setup

Figure 5.1 illustrates the transmitter testing setup. The entire assembly was mounted on a tripod (A) to ensure stable positioning during measurements. Power was supplied by a UPS, which provided a regulated 5V output with a maximum power of 15W [38]. Electrical connections were made using WAGO 3-way lever connectors.

The ultra-wideband board (C) was connected to the power amplifier (D) via SMA connectors. As both the UWB board and the amplifier featured male SMA connectors, a female-to-female SMA adapter was employed to bridge the connection. For signal attenuation during testing, attenuators (E) were inserted in the signal path[39]. Finally, the amplified signal was radiated through the antenna (F), completing the setup.

Figure 5.2 shows the receiver testing setup. The receiver system was mounted on a bicycle, which allowed the operator to quickly increase the distance to the transmitter during ranging tests. The antenna (I) was connected to the UWB board (II), which handled signal reception. Data received by the UWB board was transmitted via a USB connection (III) to a computer (IV), where it was displayed in real-time using the CoolTerm serial monitor [40].

5.2 Software setup

On the software side the transmitter configuration used during the testing was as follows:

```
static dwt_config_t config = {
    1,               /* Channel number. */
    DWT_PRF_64M,     /* Pulse repetition frequency. */
    DWT_PLEN_4096,   /* Preamble length. Used in TX only. */
    DWT_PAC64,       /* Preamble acquisition chunk size. Used in RX
       only. */
    9,               /* TX preamble code. */
    9,               /* RX preamble code. */
    1,               /* Non-standard SFD. */
    DWT_BR_110K,     /* Data rate. */
    DWT_PHRMODE_STD, /* PHY header mode. */
    (4096 + 64 - 64 + 1) /* SFD timeout. Used in RX only. */
};
```

Listing 5.1: UWB Configuration Used in Tests

This configuration prioritized extended-range communication. The parameters were specifically selected based on recommendations from the DW1000 user manual[22] and practical considerations, as described below:

- **Channel Number:**
  The channels were varied based on the tests. More on that later.
- **Pulse Repetition Frequency (PRF = 64 MHz):**
  A PRF of 64 MHz was selected to maximize receiver sensitivity. Although higher PRF consumes more power, it enhances correlation performance by increasing the number of pulses available for the receiver to integrate, thus improving detection.

- **Preamble Length (4096 symbols):**
  A preamble length of 4096 symbols was chosen to further enhance sensitivity. Longer preambles increase transmission duration and provide the receiver with a greater number of known symbols for correlation. During preliminary testing, shorter preambles resulted in higher bit error rates and reduced communication reliability, confirming that longer preambles improved overall performance.

- **Preamble Acquisition Chunk Size (PAC = 64):**
  The PAC value of 64 was selected based on the preamble length (4096 symbols), as recommended in the DW1000 user manual.

- **TX/RX Preamble Codes (Code 9):**
  Both transmitter and receiver preamble codes were set to code 9, as advised by the DW1000 user manual for configurations utilizing a 64 MHz PRF.

- **Data Rate (110 kbps):**
  A low data rate of 110 kbps was intentionally selected due to its significantly better receiver sensitivity compared to higher data rates (e.g., 6.8 Mbps). Lower data rates extend bit duration, allowing the receiver more time to integrate the signal, improving detection probability in extended-range scenarios. This effect is clearly illustrated in the DW1000 datasheet, reinforcing the decision to prioritize sensitivity over throughput[22].

- **PHY Header Mode (Standard) and SFD Timeout:**
  These parameters were left at standard recommended settings, as their effect was considered minimal.

This parameter set allowed for highest range.

During testing, the transmitter periodically sent a predefined message at approximately 420 ms intervals. The transmitted frame structure was defined as follows:

```
static uint8 tx_msg[] = {0xC5, 0x00, 'T', 'E', 'S', 'T', 0x00, 0x00};
```

Listing 5.2: Transmitted UWB Frame

The receiver was specifically configured to accept all frames, including those with errors (broken frames). Broken frames are defined as frames exhibiting errors that indicate corruption during transmission. To achieve this, the receiver monitored the DW1000 system status register (SYS_STATUS_ID), configured as:

```
while (!((status = dwt_read32bitreg(SYS_STATUS_ID)) &
         (SYS_STATUS_RXFCG | SYS_STATUS_ALL_RX_ERR)));
```

Listing 5.3: Receiver Frame Acceptance Logic

Where the error mask (SYS_STATUS_ALL_RX_ERR) is defined as:

```
#define SYS_STATUS_ALL_RX_ERR  (SYS_STATUS_RXPHE | SYS_STATUS_RXFCE |
    SYS_STATUS_RXRFSL | SYS_STATUS_RXSFDTO | SYS_STATUS_AFFREJ |
   SYS_STATUS_LDEERR)
```

Listing 5.4: RX Error Mask Definition

Each status bit has the following meaning, according to the DW1000 user manual[22]:

- `SYS_STATUS_RXFCG`: Receiver FCS good (valid checksum)
- `SYS_STATUS_RXPHE`: PHY header error
- `SYS_STATUS_RXFCE`: Frame checksum error (FCS error)
- `SYS_STATUS_RXRFSL`: Receiver Reed Solomon frame length error
- `SYS_STATUS_RXSFDTO`: Receiver SFD timeout
- `SYS_STATUS_AFFREJ`: Automatic frame filtering rejection
- `SYS_STATUS_LDEERR`: Leading edge detection error

Bit Error Rate (BER) was calculated only for frames with the correct expected length (8 bytes). To exclude the two checksum bytes (FCS), only the first 6 bytes of payload data were evaluated. The calculation was performed using the bitwise XOR operation to detect differences between received and expected messages:

```
for (int i = 0; i < EXPECTED_FRAME_LEN - 2; i++) {
    uint8_t rx_byte = (i < frame_len) ? rx_buffer[i] : 0x00;
    uint8_t xor_byte = rx_byte ^ expected_msg[i];
    for (int b = 0; b < 8; b++) {
        if (!(xor_byte & (1 << b))) {
            match_bits++;
        }
    }
}

float ber = 100.0f * (1.0f - (float)match_bits / expected_bits);
```

Listing 5.5: Bit Error Calculation

Here, `match_bits` represents the count of matching bits, and `expected_bits` is the total number of bits evaluated (48 bits for the 6-byte payload). The resulting BER percentage shows the proportion of incorrect bits received in the transmitted frames. This provides a quantitative measure for bit errors.

5.3 Testing Conditions and Methodology

The objective of the testing was to determine the maximum practical communication range of the custom UWB system under real-world outdoor conditions. The transmitter (TX) remained stationary and continuously broadcasted packets at fixed intervals of approximately 420 ms. The

receiver (RX) was gradually moved away from the TX, and at each arbitrary test point, the reception of valid data packets was manually verified.

At each location, the RX was held for 120 seconds. During this period, if at least one valid/invalid data packet, the distance was considered valid and testing continued at a further location. If no packets were received within the observation window, the RX was moved back to the last location where successful reception occurred, and that position was recorded as the maximum communication range. All distance measurements were recorded using the Geo Tracker [41] application.

To improve packet detection, the RX antenna was manually rotated during each test interval, introducing possible reception variation. This action was not standardized, and the extent to which it influenced results is unknown, as the real-world radiation pattern of the antenna is not characterized.

The elevation of the RX varied slightly due to terrain, with an estimated maximum variation of ±3 meters. The TX, however, was fixed in both position and elevation throughout the experiment. The 2-minute observation period was arbitrarily chosen.

The criteria for accepting a range as valid was the successful reception of at least one data packet. BER was not used as a limiting factor, as no bit errors were observed at longer distances; instead, packet loss became the primary constraint.

5.4 Results

5.4.1 Effect of Amplification

To evaluate the effect of transmit power on communication range, tests were conducted using the custom UWB board both with and without amplification. Without the amplifier, the system achieved a maximum range of approximately 70 meters. This is lower than the range of up to 290 meters specified in the DW1000 datasheet for a 110 kbps data rate[22]. With the amplifier, three attenuation settings were tested: 20 dB, 10 dB, and 0 dB.

All attenuation tests were performed on UWB Channel 1, which has a bandwidth of 499.2 MHz. The DW1000 transceiver provides programmable transmit power, with typical default output power spectral density in the range of -39 to $-35\,\mathrm{dBm/MHz}$ [22]. With a measured amplifier gain of $25.5\,\mathrm{dB} \pm 0.52\,\mathrm{dB}$, the effective output power at the antenna port (neglecting cable and connector losses) is shown in Table 5.1.

The default transmit power register value is `0x1E080222`, which corresponds to an output of approximately $-14\,\mathrm{dBm}$. This value is specified also in the product brief[42]. This is based on Decawave's default values[22].

The measured impact of transmit power on communication range is summarized in Table 5.1. As expected, increased attenuation leads to reduced range.

Table 5.1: Amplifier Attenuation, Output Power and Measured Maximum Range (Channel 1)

Attenuation (dB)	Output Power (dBm)	Max Range (m)
20	-8.5	289
10	1.5	580
0	11.5	1290

5.4.2 Channel Comparison

Following the evaluation of transmit power effects on range, additional tests were carried out to compare the range performance across different UWB channels. All measurements were conducted using the same test environment, antenna setup, and with 0 dB attenuation (maximum amplification scenario). The purpose of this comparison was to observe how different UWB frequency bands affect propagation characteristics and maximum achievable range.

Channels 1 to 3 utilize frequencies in the 3.5–4.5 GHz range with a 499.2 MHz bandwidth. Although Channel 4 nominally spans a wider 1331.2 MHz frequency range centered at 3993.6 MHz, the DW1000 transceiver was not reconfigured to use the optional 900 MHz receive bandwidth mode. Therefore, the default 499.2 MHz bandwidth setting was used for both transmission and reception [43].

Longer ranges generally benefit from lower frequencies due to reduced free-space path loss. In this case, Channel 4 significantly outperformed the others, reaching a maximum measured distance of 2.63 km under line-of-sight conditions. This is likely due to better matching with the antenna and amplifier system used.

Table 5.2 summarizes the observed maximum range for each tested channel.

Table 5.2: Range Comparison Across Channels (0 dB Attenuation)

Channel	Max Range (m)
1	1290
2	1200
3	1100
4	2630

5.4.3 Observations

BER was observed to be relatively high at short ranges, specifically when the distance between the transmitter and receiver was less than 50 meters both with and without the amplifier. This can be likely attributed to environmental reflections. Another possible explanation is that amplifier at the receiver may have been overloaded at these short distances. The exact cause remains undetermined.

At longer distances, near the system's maximum communication distance, packet loss emerged as the primary limitation. However, the packets that were successfully received did not have any bit errors. This behavior shows an abrupt transition between fully reliable reception and

complete communication failure. One potential explanation is the short packet length used during testing — only 8 bytes, of which a large portion constituted protocol overhead. This high relative overhead may have contributed to the observed transmission characteristics. Further investigation is required to confirm this hypothesis.

6 Conclusion

This thesis demonstrated the feasibility of using UWB radio for extended-range communication in outdoor environments. A custom platform was developed, consisting of a DW1000-based transceiver, a high-gain power amplifier, and an antenna. Field tests showed that with proper hardware design and configuration, communication distances of up to 2.6 km can be achieved—far exceeding typical UWB usage ranges.

Throughout testing, the bit error rate remained low at long distances. The main limiting factor was packet loss, which became dominant near the system's maximum range. Notably, successfully received packets contained no bit errors, indicating a sharp transition from reliable communication to complete loss. This suggests that UWB signal integrity is preserved until the signal drops below the reception threshold.

Future work could include characterization of the antenna's radiation pattern and evaluation under controlled multipath conditions. Further improvements may also involve real-time localization and multi-node communication in more dynamic scenarios.

In summary, UWB can be effectively used for extended-range outdoor communication. The platform developed here offers a practical and flexible basis for further applied research and system development.

Acknowledgments

I would like to thank my supervisor Jaanus Kalde for his guidance during this thesis and for sparking my interest in radio technology. Also, I want to thank Institute of Technology and InFTF for supporting this work financially.

Bibliography

[1] *Robot navigation*, in *Wikipedia*, Page Version ID: 1267450465, Jan. 5, 2025. [Online]. Available: https://en.wikipedia.org/w/index.php?title=Robot_navigation&oldid=1267450465 (visited on 03/24/2025).

[2] "Data challenges in autonomous driving: Regional insights." (), [Online]. Available: https://www.sapien.io/blog/global-autonomous-driving-readiness-regional-data-challenges?utm_source=chatgpt.com (visited on 05/15/2025).

[3] S. Wang and N. S. Ahmad, "AI-based approaches for improving autonomous mobile robot localization in indoor environments: A comprehensive review," *Engineering Science and Technology, an International Journal*, vol. 63, p. 101 977, Mar. 1, 2025, ISSN: 2215-0986. DOI: 10.1016/j.jestch.2025.101977. [Online]. Available: https://www.sciencedirect.com/science/article/pii/S2215098625000321 (visited on 05/15/2025).

[4] G. MacGougan, G. Lachapelle, R. Nayak, and A. Wang, "Overview of GNSS signal degradation phenomena," 2001.

[5] ERR. "GPS-signaalide häirimine Venemaa poolt on Eesti kohal suurenenud," ERR. Section: Eesti. (Apr. 4, 2024), [Online]. Available: https://www.err.ee/1609302099/gps-signaalide-hairimine-venemaa-poolt-on-eesti-kohal-suurenenud (visited on 03/23/2025).

[6] Qorvo. "Getting back to basics with ultra-wideband (UWB)." (2021), [Online]. Available: https://www.qorvo.com/resources/d/qorvo-getting-back-to-basics-with-ultra-wideband-uwb-white-paper (visited on 03/24/2025).

[7] M. F. R. Al-Okby, S. Junginger, T. Roddelkopf, and K. Thurow, "UWB-based real-time indoor positioning systems: A comprehensive review," *Applied Sciences*, vol. 14, no. 23, p. 11 005, Jan. 2024, Number: 23 Publisher: Multidisciplinary Digital Publishing Institute, ISSN: 2076-3417. DOI: 10.3390/app142311005. [Online]. Available: https://www.mdpi.com/2076-3417/14/23/11005 (visited on 05/05/2025).

[8] Ł. Rykała, A. Typiak, and R. Typiak, "Research on developing an outdoor location system based on the ultra-wideband technology," *Sensors*, vol. 20, no. 21, p. 6171, Oct. 29, 2020, ISSN: 1424-8220. DOI: 10.3390/s20216171. [Online]. Available: https://www.mdpi.com/1424-8220/20/21/6171 (visited on 03/25/2025).

[9] J. Xia, C. L. Law, Y. Zhou, and K. S. Koh, "3–5 GHz UWB impulse radio transmitter and receiver MMIC optimized for long range precision wireless sensor networks," *IEEE Transactions on Microwave Theory and Techniques*, p. 5 608 531, Dec. 2010, ISSN: 0018-9480, 1557-9670. DOI: 10.1109/TMTT.2010.2083682. [Online]. Available: http://ieeexplore.ieee.org/document/5608531/ (visited on 03/25/2025).

[10] B. Van Herbruggen, B. Jooris, J. Rossey, *et al.*, "Wi-PoS: A low-cost, open source ultra-wideband (UWB) hardware platform with long range sub-GHz backbone," *Sensors*, vol. 19, no. 7, p. 1548, Mar. 30, 2019, ISSN: 1424-8220. DOI: 10.3390/s19071548. [Online]. Available: https://www.mdpi.com/1424-8220/19/7/1548 (visited on 03/25/2025).

[11] K. S. PhD. "How far are we from level 5 autonomy?" (Dec. 14, 2022), [Online]. Available: https://blog.guardknox.com/how-far-are-we-from-level-5-autonomy (visited on 03/24/2025).

[12] "Autonomous vehicle market size, share, trends | report [2030]." (), [Online]. Available: https://www.fortunebusinessinsights.com/autonomous-vehicle-market-109045 (visited on 03/24/2025).

[13] M. Alam. "Localization in robotics for mobile robots," Medium. (Oct. 3, 2023), [Online]. Available: https://medium.com/@mansooralam129047/localization-in-robotics-for-mobile-robots-ec3ad31f99d4 (visited on 03/24/2025).

[14] ERR. "GPS-signaalide häirimine Venemaa poolt on Eesti kohal suurenenud," ERR. Section: Eesti. (Apr. 4, 2024), [Online]. Available: https://www.err.ee/1609641395/suurem-hambaravihuvitis-kasvatas-huvi-hambaarsti-kulastada (visited on 03/23/2025).

[15] "High-rate RTK: Helpful or hypeful?" GPS World. Section: Featured Stories. (Jan. 13, 2022), [Online]. Available: https://www.gpsworld.com/high-rate-rtk-helpful-or-hypeful/ (visited on 03/24/2025).

[16] "LiDAR-based sensor fusion SLAM and localization for autonomous driving vehicles in complex scenarios." (), [Online]. Available: https://www.mdpi.com/2313-433X/9/2/52?utm_source=chatgpt.com (visited on 03/24/2025).

[17] M. Bizzaco. "Does the samsung SmartTag 2 have UWB?" Android Police. Section: Accessories. (Nov. 16, 2023), [Online]. Available: https://www.androidpolice.com/samsung-smarttag-2-uwb/ (visited on 03/24/2025).

[18] "What is ultra-wideband (UWB) wireless communication? | murata manufacturing articles." (Sep. 27, 2023), [Online]. Available: https://article.murata.com/en-global/article/what-is-uwb-wireless-communication (visited on 03/24/2025).

[19] "EVK1000 - qorvo." (), [Online]. Available: https://www.qorvo.com/products/p/https//www.qorvo.com/products/p/EVK1000 (visited on 04/09/2025).

[20] "DWM3001cdk - qorvo." (), [Online]. Available: https://www.qorvo.com/products/p/https//www.qorvo.com/products/p/DWM3001CDK (visited on 04/08/2025).

[21] "DWM3000evb - qorvo." (), [Online]. Available: https://www.qorvo.com/products/p/https//www.qorvo.com/products/p/DWM3000EVB (visited on 04/08/2025).

[22] Decawave, *DW1000 data sheet*. [Online]. Available: https://www.qorvo.com/products/d/da007946.

[23] "EVK-SR1010-MP1/SR1020-MP1 ultra-low-power, short-latency wireless SPARK UWB evaluation kits," DigiKey. (), [Online]. Available: https://www.digikey.ee/en/product-highlight/s/spark-microsystems/evk-sr1010-mp1-and-evk-sr1020-mp1-uwb-evaluation-kit (visited on 04/08/2025).

[24] "QM33120wdk1 - qorvo." (), [Online]. Available: https://www.qorvo.com/products/p/https//www.qorvo.com/products/p/QM33120WDK1 (visited on 04/08/2025).

[25] "DWM1000_data_sheet-1950396." (), [Online]. Available: https://www.mouser.ee/datasheet/2/412/DWM1000_Data_Sheet-1950396.pdf (visited on 04/08/2025).

[26] "DWM3000_data_sheet_brief-2399958." (), [Online]. Available: https://www.mouser.ee/datasheet/2/412/DWM3000_Data_Sheet_Brief-2399958.pdf (visited on 04/08/2025).

[27] R. S. G. KG. C. "R&s®ZND vector network analyzers." (), [Online]. Available: https://www.rohde-schwarz.com/ae/products/test-and-measurement/network-analyzers/rs-znd-vector-network-analyzers_63493-65409.html (visited on 04/09/2025).

[28] "Male SMA SOL 4 pcs calibration kit of premium 12 GHz parts in wooden box by SDR-kits." (), [Online]. Available: https://www.sdr-kits.net/Male-12GHz-Kit (visited on 04/09/2025).

[29] "A49t 5v 20 DB RF broad band low noise amplifier module 0.05-6g high-linearity high gain LNA amp board RF FM HF VHF," aliexpress. (), [Online]. Available: //www.aliexpress.com/item/1005008565792621.html?src=ibdm_d03p0558e02r02&sk=&aff_platform=&aff_trace_key=&af=&cv=&cn=&dp=&aff_short_key= (visited on 04/09/2025).

[30] "DEEPACE wideband omnidirectional antenna UWB-1 3.1ghz-9ghz | DEEPACE |." (), [Online]. Available: https://deepace.net/product/uwb-1-3-1ghz-9ghz-wideband-omnidirectional-antenna/ (visited on 04/09/2025).

[31] "DEEPACE wideband omnidirectional antenna UWB-2 2.8ghz-11ghz | DEEPACE |." (), [Online]. Available: https://deepace.net/product/uwb-2-2-8ghz-11ghz-wideband-omnidirectional-antenna/ (visited on 04/09/2025).

[32] "Qorvo_dw3000-2934245." (), [Online]. Available: https://www.mouser.com/datasheet/2/412/Qorvo_DW3000-2934245.pdf?srsltid=AfmBOorKqiNzAoTcrGhNbZA3lYIRrs (visited on 04/08/2025).

[33] Spark. "Datasheet_sr1010_customer." (), [Online]. Available: https://www.sparkmicro.com/wp-content/uploads/2024/03/datasheet_SR1010_customer.pdf (visited on 04/08/2025).

[34] "Datasheet_sr1020_v1.02." (), [Online]. Available: https://www.sparkmicro.com/wp-content/uploads/2021/11/datasheet_SR1020_V1.02.pdf (visited on 04/08/2025).

[35] "Exploring ultra-wideband technology for micro-location-based services - page 2 | microwave journal." (), [Online]. Available: https://www.microwavejournal.com/articles/36143-exploring-ultra-wideband-technology-for-micro-location-based-services?page=2 (visited on 04/08/2025).

[36] "F1485 - high gain RF amplifier 2300mhz to 5000mhz | renesas." (), [Online]. Available: https://www.renesas.com/en/products/rf-products/rf-amplifiers/f1485-high-gain-rf-amplifier-2300mhz-5000mhz (visited on 04/12/2025).

[37] N. Suguna and R. Senthil, "Split–ring resonator loaded pentagon antenna for super wide band communications," *Materials Today: Proceedings*, Mar. 21, 2023, ISSN: 2214-7853. DOI: 10.1016/j.matpr.2023.02.420. [Online]. Available: https://www.sciencedirect.com/science/article/pii/S2214785323009859 (visited on 04/13/2025).

[38] "Type-c 15w 3a fast charge UPS power supply / 18650 lithium battery charger module DC-DC step up booster converter 5v 9v 12v," aliexpress. (), [Online]. Available: //www.aliexpress.com/item/1005008627038579.html?src=ibdm_d03p0558e02r02&sk=&aff_platform=&aff_trace_key=&af=&cv=&cn=&dp=&aff_short_key= (visited on 04/04/2025).

[39] "10 dB - fixed attenuator SMA male to SMA female up to 6 GHz rated to 2 watts with round hex passivated stainless steel body," HASCO COMPONENTS. (), [Online]. Available: https://www.hasco-inc.com/attenuators/10-db-fixed-attenuator-sma-male-to-sma-female-up-to-6-ghz-rated-to-2-watts-with-round-hex-passivated-stainless-steel-body/ (visited on 04/07/2025).

[40] "CoolTerm," LO4D.com. (), [Online]. Available: https://coolterm.en.lo4d.com/windows (visited on 04/07/2025).

[41] "Geo tracker - GPS tracker (en)." (), [Online]. Available: https://geo-tracker.org/en (visited on 04/04/2025).

[42] *DW1000 product brief (1)*, Jun. 5, 2025. [Online]. Available: https://www.qorvo.com/products/d/da007945.

[43] Decawave, *DW1000 user manual*. [Online]. Available: https://www.qorvo.com/products/d/da007967.

Appendix

I. UWB Board Schematic

Version 0.0:
This PCB MUST BE manufactured according to spec JLC04161H-3313

Version 0.1 :
This PCB MUST BE manufactured according to spec JLC04161H-7628
JTAG valesti
NRST to 470ohm stm32
D+ pull-up to 1.5kOhm
GPIO to NRST on DW1000 (high Z and pull low)
Removed supervisor near dw1000
DW1000 clk configurability
SPI conf pulled (both) pulled 0
Stackup- change

U_Top
Top.SchDoc

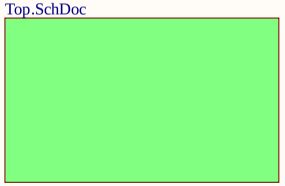

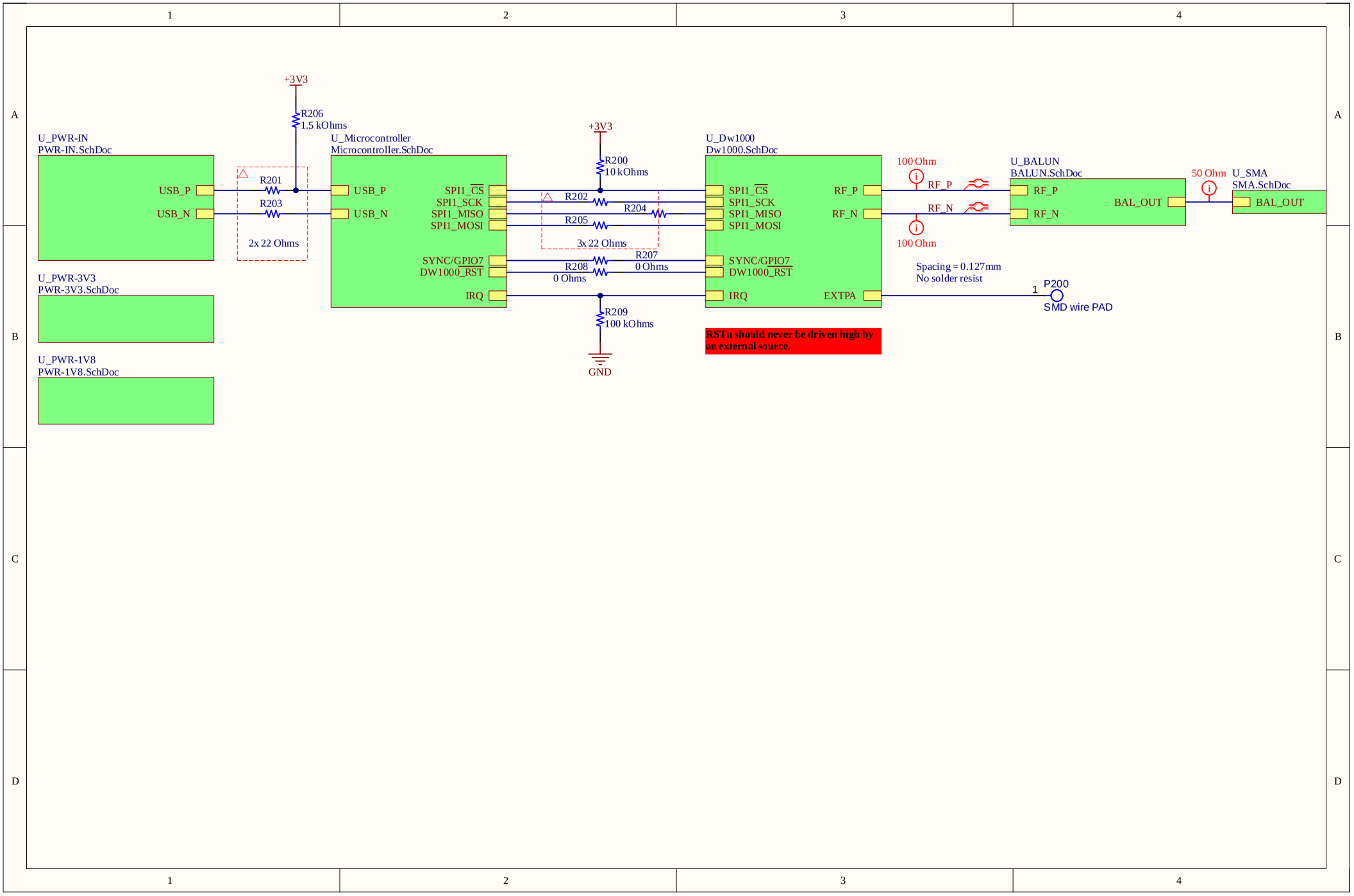
+3V3
R206
1.5 kOhms
U_PWR-IN
PWR-IN.SchDoc
USB_P
USB_N
R201
R203
2x 22 Ohms
U_Microcontroller
Microcontroller.SchDoc
USB_P
USB_N
SPI1_CS
SPI1_SCK
SPI1_MISO
SPI1_MOSI
SYNC/GPIO7
DW1000_RST
IRQ
+3V3
R200
10 kOhms
R202
R204
R205
3x 22 Ohms
R207
0 Ohms
R208
0 Ohms
R209
100 kOhms
GND
U_Dw1000
Dw1000.SchDoc
SPI1_CS
SPI1_SCK
SPI1_MISO
SPI1_MOSI
SYNC/GPIO7
DW1000_RST
IRQ
RF_P
RF_N
EXTPA
RSTn should never be driven high by an external source.
100 Ohm
RF_P
RF_N
100 Ohm
U_BALUN
BALUN.SchDoc
RF_P
RF_N
BAL_OUT
50 Ohm
U_SMA
SMA.SchDoc
BAL_OUT
Spacing = 0.127mm
No solder resist
1
P200
SMD wire PAD
U_PWR-3V3
PWR-3V3.SchDoc
U_PWR-1V8
PWR-1V8.SchDoc

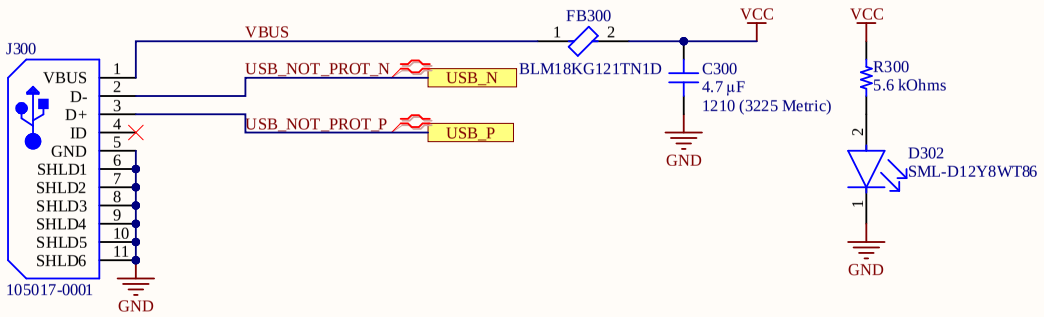
J300
VBUS
D-
D+
ID
GND
SHLD1
SHLD2
SHLD3
SHLD4
SHLD5
SHLD6
1
2
3
4
5
6
7
8
9
10
11
105017-0001
GND
VBUS
USB_NOT_PROT_N
USB_N
USB_NOT_PROT_P
USB_P
FB300
1
2
BLM18KG121TN1D
VCC
C300
4.7 µF
1210 (3225 Metric)
GND
VCC
R300
5.6 kOhms
2
1
D302
SML-D12Y8WT86
GND

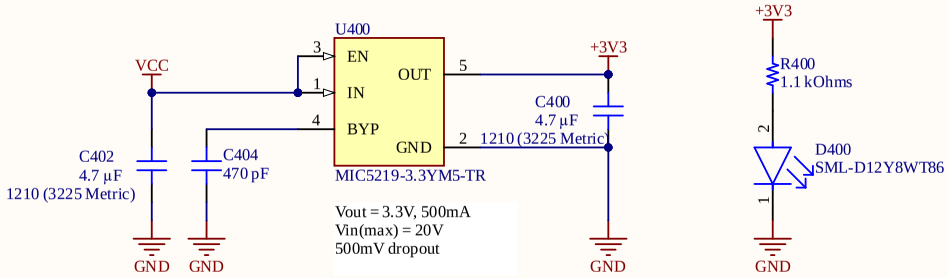
U400
EN
IN
BYP
OUT
GND
3
1
4
5
2
VCC
+3V3
C402
4.7 µF
1210 (3225 Metric)
C404
470 pF
C400
4.7 µF
1210 (3225 Metric)
MIC5219-3.3YM5-TR
Vout = 3.3V, 500mA
Vin(max) = 20V
500mV dropout
GND
GND
GND

+3V3
R400
1.1 kOhms
D400
SML-D12Y8WT86
2
1
GND

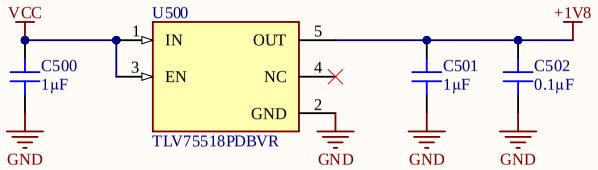
VCC
U500
+1V8
IN
OUT
EN
NC
GND
TLV75518PDBVR
C500
1µF
C501
1µF
C502
0.1µF
GND
GND
GND
GND

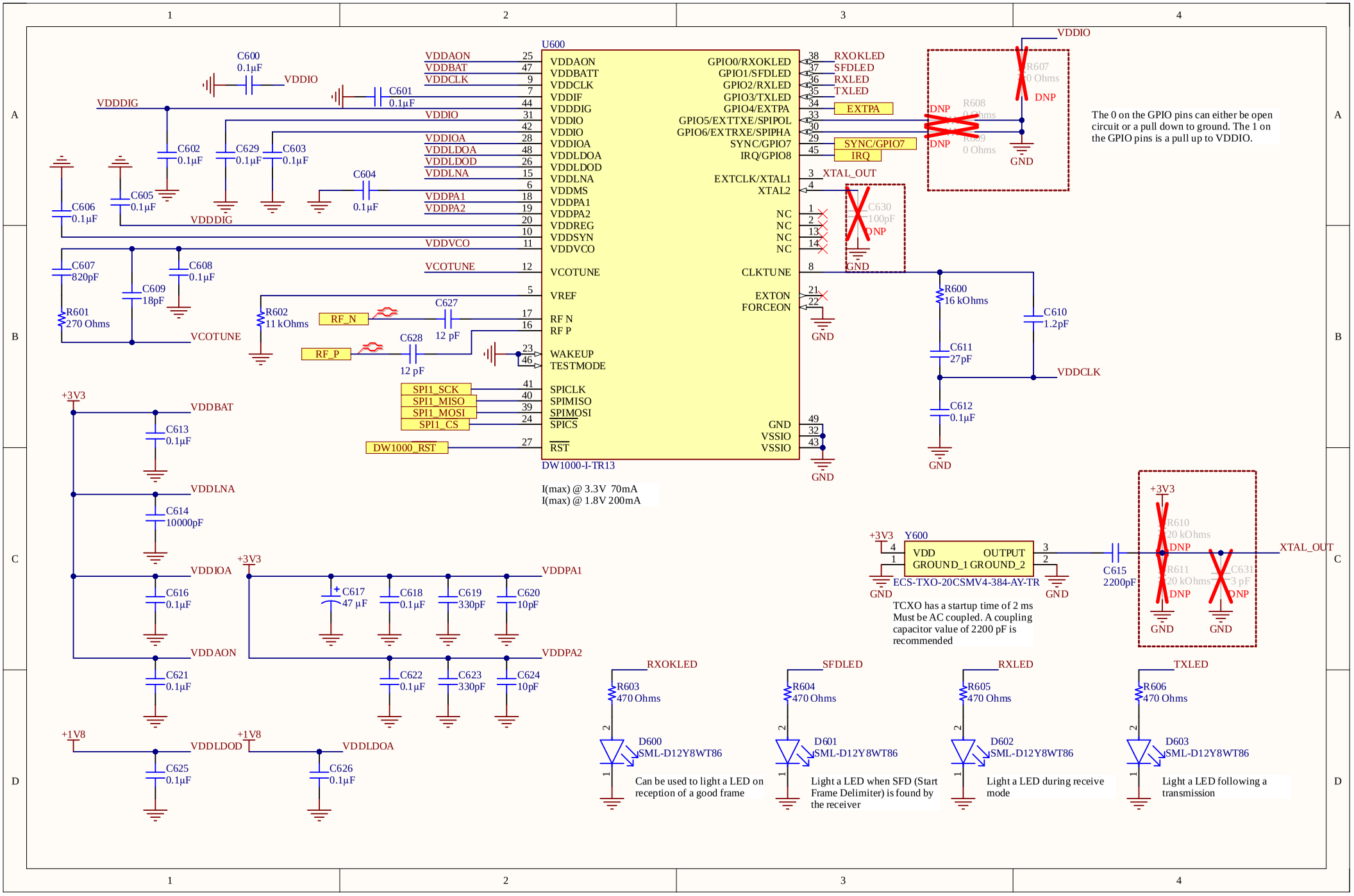
U600
DW1000-I-TR13
VDDAON
VDDBAT
VDDCLK
VDDIF
VDDDIG
VDDIO
VDDIOA
VDDLDOA
VDDLDOD
VDDLNA
VDDMS
VDDPA1
VDDPA2
VDDREG
VDDSYN
VDDVCO
VCOTUNE
VREF
RF N
RF P
WAKEUP
TESTMODE
SPICLK
SPIMISO
SPIMOSI
SPICS
RST
GPIO0/RXOKLED
GPIO1/SFDLED
GPIO2/RXLED
GPIO3/TXLED
GPIO4/EXTPA
GPIO5/EXTTXE/SPIPOL
GPIO6/EXTRXE/SPIPHA
SYNC/GPIO7
IRQ/GPIO8
EXTCLK/XTAL1
XTAL2
NC
CLKTUNE
EXTON
FORCEON
GND
VSSIO
RXOKLED
SFDLED
RXLED
TXLED
EXTPA
SYNC/GPIO7
IRQ
XTAL_OUT
SPI1_SCK
SPI1_MISO
SPI1_MOSI
SPI1_CS
DW1000_RST
I(max) @ 3.3V 70mA
I(max) @ 1.8V 200mA
The 0 on the GPIO pins can either be open circuit or a pull down to ground. The 1 on the GPIO pins is a pull up to VDDIO.
R607 330 Ohms
R608 0 Ohms
R609 0 Ohms
DNP
C600 0.1µF
C601 0.1µF
C602 0.1µF
C603 0.1µF
C604 0.1µF
C605 0.1µF
C606 0.1µF
C607 820pF
C608 0.1µF
C609 18pF
C610 1.2pF
C611 27pF
C612 0.1µF
C613 0.1µF
C614 10000pF
C615 2200pF
C616 0.1µF
C617 47 µF
C618 0.1µF
C619 330pF
C620 10pF
C621 0.1µF
C622 0.1µF
C623 330pF
C624 10pF
C625 0.1µF
C626 0.1µF
C627 12 pF
C628 12 pF
C629 0.1µF
C630 100pF
C631 3 pF
R600 16 kOhms
R601 270 Ohms
R602 11 kOhms
R603 470 Ohms
R604 470 Ohms
R605 470 Ohms
R606 470 Ohms
R610 20 kOhms
R611 20 kOhms
Y600
VDD
OUTPUT
GROUND_1
GROUND_2
ECS-TXO-20CSMV4-384-AY-TR
TCXO has a startup time of 2 ms
Must be AC coupled. A coupling capacitor value of 2200 pF is recommended
D600 SML-D12Y8WT86
D601 SML-D12Y8WT86
D602 SML-D12Y8WT86
D603 SML-D12Y8WT86
Can be used to light a LED on reception of a good frame
Light a LED when SFD (Start Frame Delimiter) is found by the receiver
Light a LED during receive mode
Light a LED following a transmission
+3V3
+1V8
VDDBAT
VDDLNA
VDDIOA
VDDAON
VDDLDOD
VDDLDOA
VDDPA1
VDDPA2
VDDIO
VDDDIG
VDDVCO
VCOTUNE
VDDCLK
RF_N
RF_P

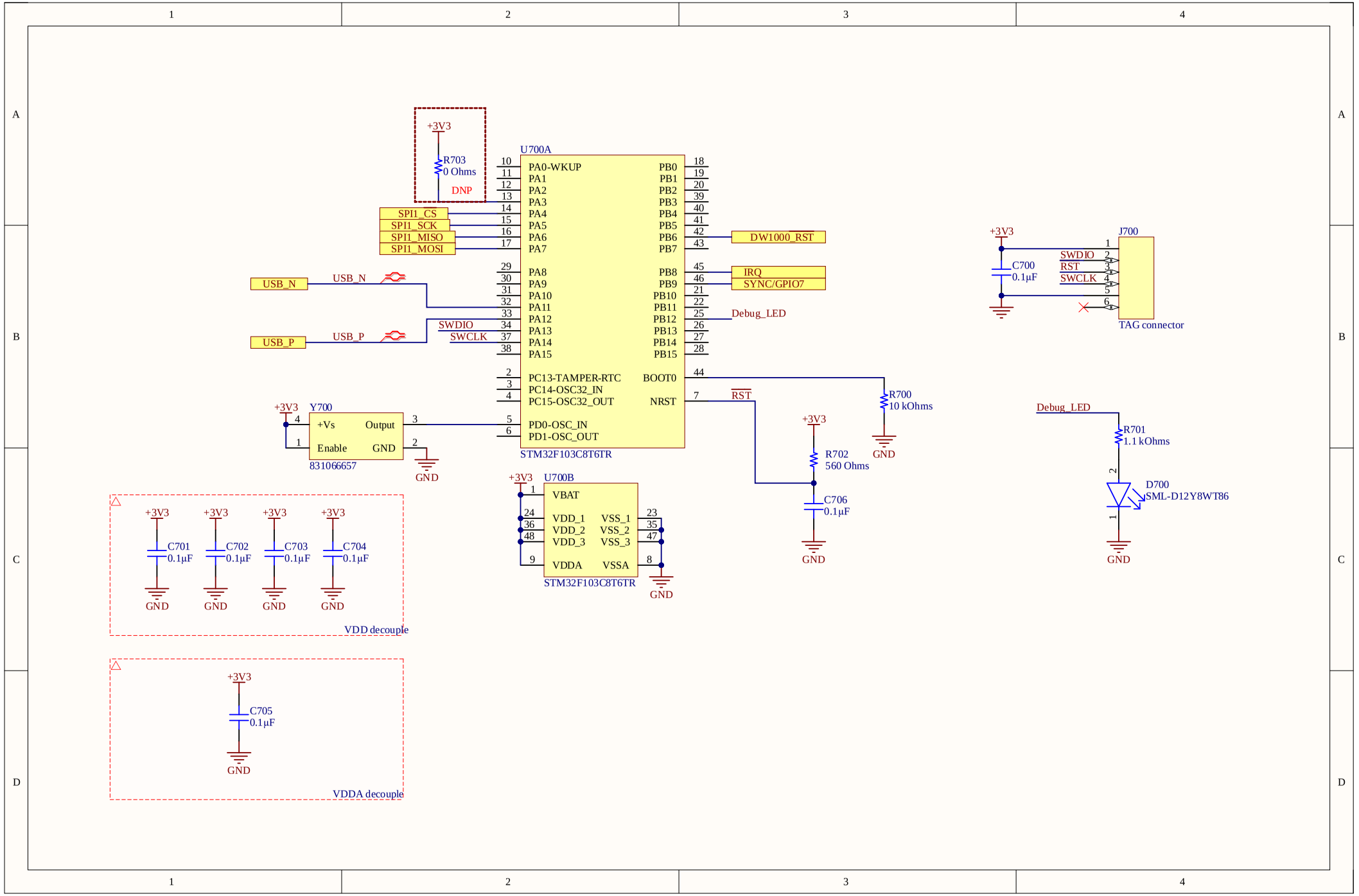
+3V3
R703
0 Ohms
DNP
U700A
PA0-WKUP
PA1
PA2
PA3
PA4
PA5
PA6
PA7
PA8
PA9
PA10
PA11
PA12
PA13
PA14
PA15
PC13-TAMPER-RTC
PC14-OSC32_IN
PC15-OSC32_OUT
PD0-OSC_IN
PD1-OSC_OUT
PB0
PB1
PB2
PB3
PB4
PB5
PB6
PB7
PB8
PB9
PB10
PB11
PB12
PB13
PB14
PB15
BOOT0
NRST
STM32F103C8T6TR
SPI1_CS
SPI1_SCK
SPI1_MISO
SPI1_MOSI
DW1000_RST
IRQ
SYNC/GPIO7
Debug_LED
USB_N
USB_P
SWDIO
SWCLK
RST
R700
10 kOhms
R702
560 Ohms
C706
0.1µF
Y700
+Vs
Output
Enable
GND
831066657
U700B
VBAT
VDD_1
VDD_2
VDD_3
VDDA
VSS_1
VSS_2
VSS_3
VSSA
STM32F103C8T6TR
C700
0.1µF
J700
SWDIO
RST
SWCLK
TAG connector
R701
1.1 kOhms
D700
SML-D12Y8WT86
C701
C702
C703
C704
0.1µF
VDD decouple
C705
VDDA decouple

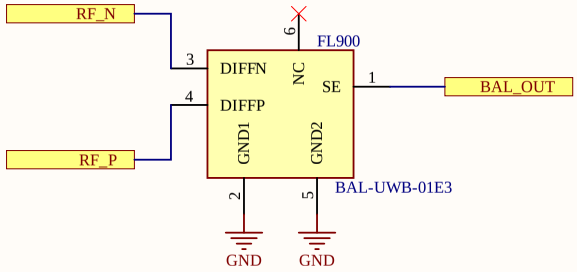
RF_N
RF_P
3
4
6
FL900
DIFFN
DIFFP
NC
SE
GND1
GND2
1
BAL_OUT
BAL-UWB-01E3
2
5
GND
GND

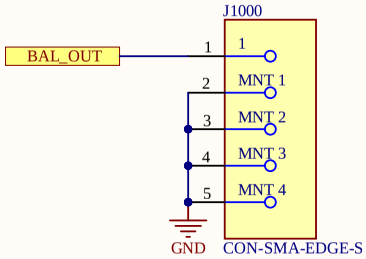
J1000
BAL_OUT
1
1
2
MNT 1
3
MNT 2
4
MNT 3
5
MNT 4
GND
CON-SMA-EDGE-S

II. UWB Board PCB

Top, Inner 1, Inner 2, Bottom and Overlay layers are shown.

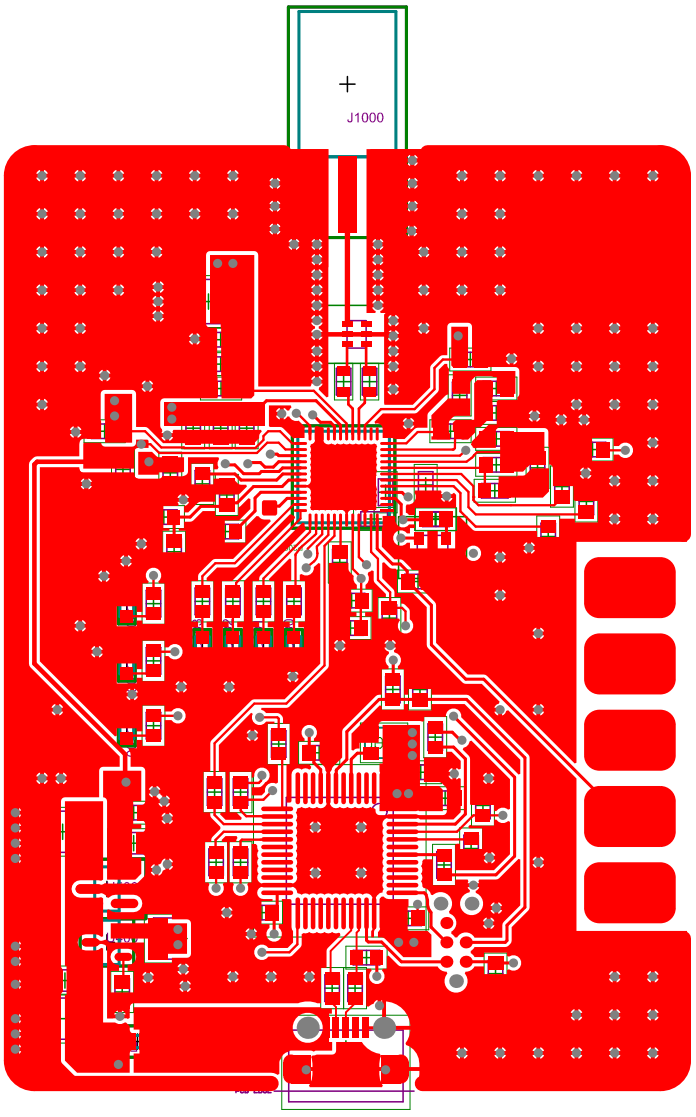
J1000

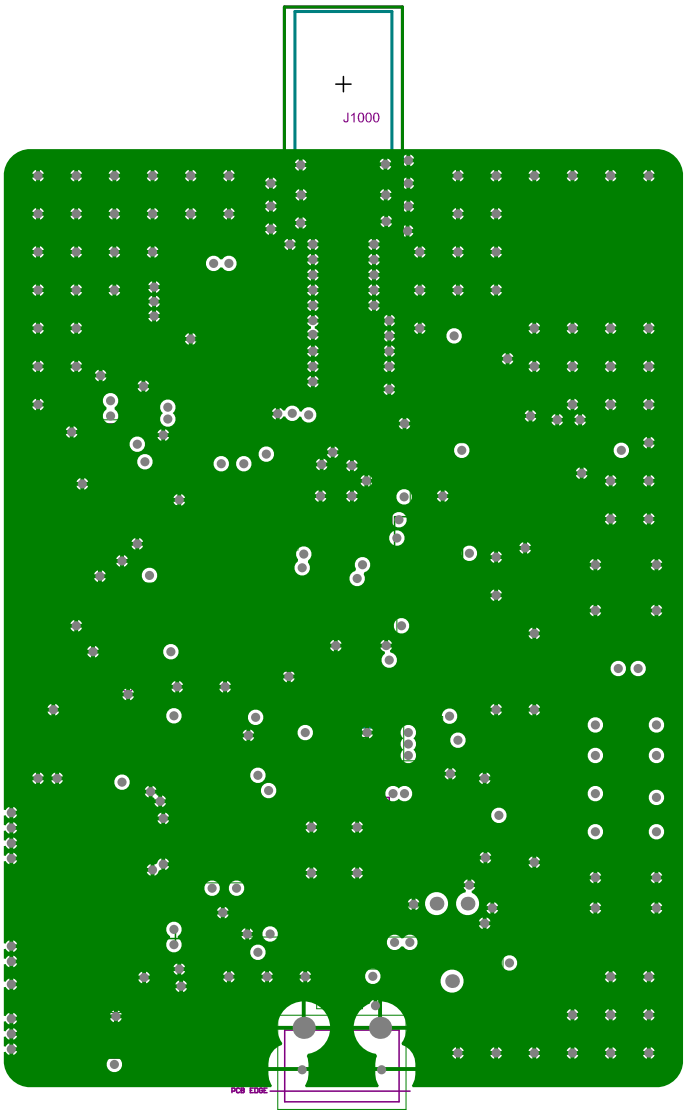
J1000
PCB EDGE

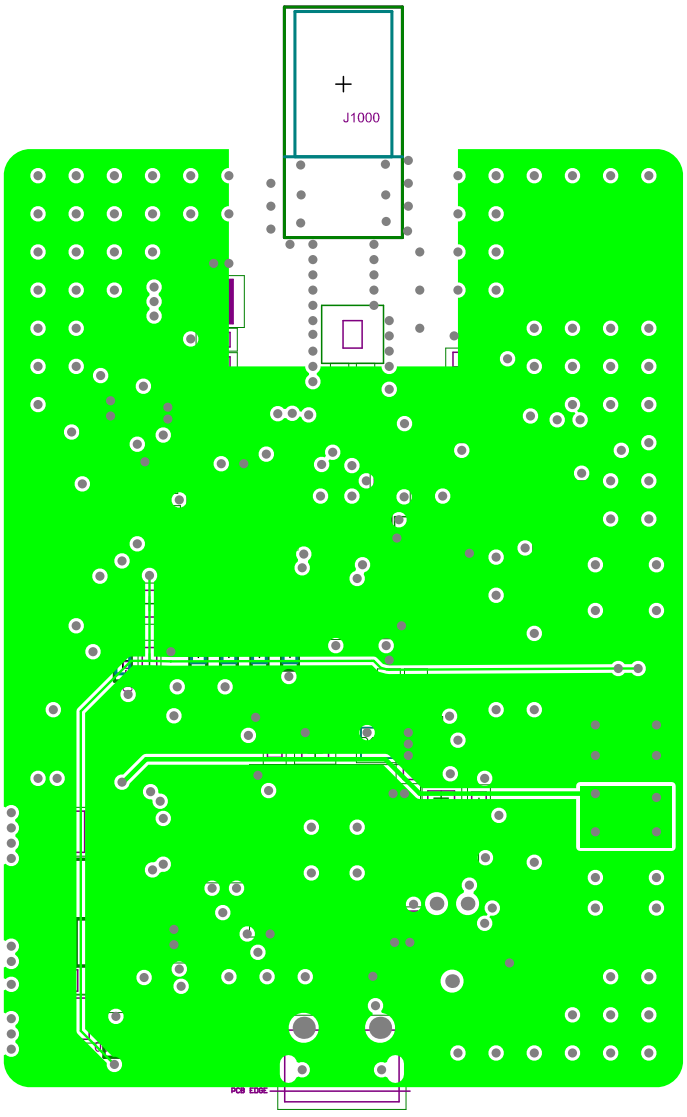
J1000
PCB EDGE

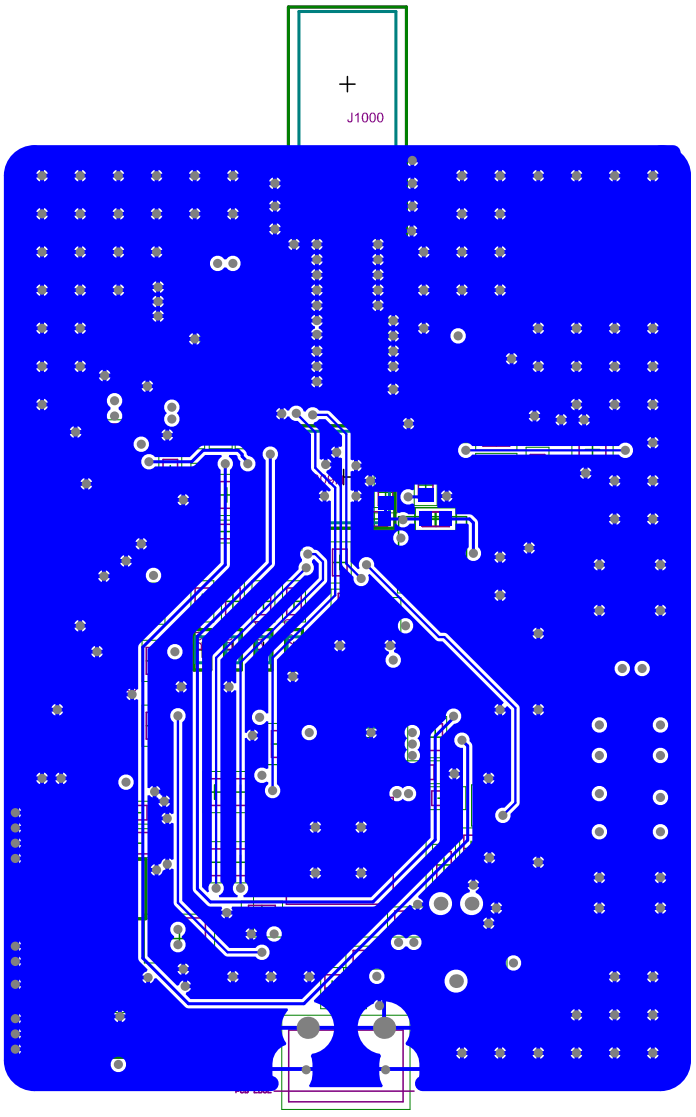
J1000

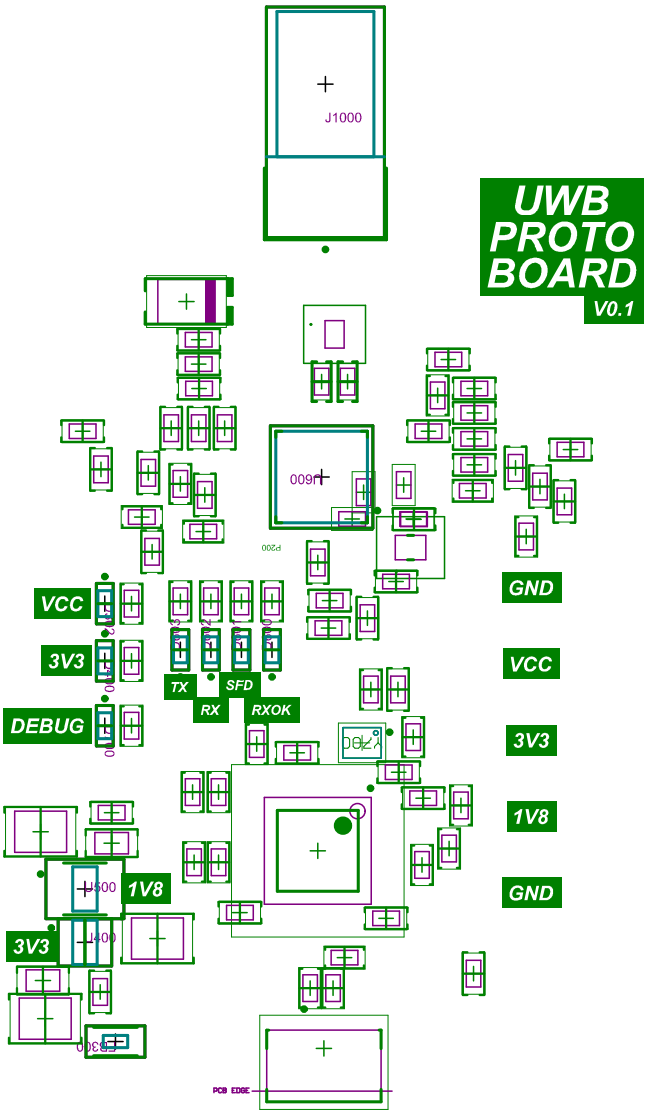
J1000
UWB
PROTO
BOARD
V0.1
J600
P200
VCC
3V3
DEBUG
TX
RX
SFD
RXOK
GND
VCC
3V3
1V8
GND
J500
1V8
J400
3V3
C330
PCB EDGE

III. UWB Board Bill of Materials

Name	Description	Designator(s)	Qty
CL32B475KBUYNNE	CAP CER 4.7UF 50V X7R 1210	C300, C400, C402	3
0603B471K101CT	CAP CER 470PF 100V X7R 0603	C404	1
0805ZC105KAT4A	CAP CER 1UF 10V X7R 0805	C500, C501	2
06035C104MAT2A	CAP CER 0.1UF 50V X7R 0603	C502, C600, C601, C602, C603, C604, C605, C606, C608, C612, C613, C616, C618, C621, C622, C625, C626, C629, C700, C701, C702, C703, C704, C705, C706	25
06035A821JAT2A	CAP CER 820PF 50V C0G/NP0 0603	C607	1
06035A180JAT4A	CAP CER 18PF 50V NP0 0603	C609	1
06035A1R2K4T2A	CAP CER 1.2PF 50V C0G/NP0 0603	C610	1
06035A270JAT2A	CAP CER 27PF 50V C0G/NP0 0603	C611	1
06035C103KAT2A	CAP CER 10000PF 50V X7R 0603	C614	1
06033C222JAT2A	CAP CER 2200PF 25V X7R 0603	C615	1
T494B476K010AT	CAP TANT 47UF 10% 10V 1411	C617	1
06035C331K4T2A	CAP CER 330PF 50V X7R 0603	C619, C623	2
06035A100JAT2A	CAP CER 10PF 50V C0G/NP0 0603	C620, C624	2
12 pF	CAP CER 12PF 100V C0G/NP0 0603	C627, C628	2
SML-D12Y8WT86	LED YELLOW DIFFUSED 0603 SMD	D302, D400, D600, D601, D602, D603, D700	7
BLM18KG121TN1D	FERRITE BEAD 120 OHM 0603 1LN	FB300	1

Continued on next page

Name	Description	Designator(s)	Qty
BAL-UWB-01E3	Filter	FL900	1
105017-0001	Micro-USB B Receptacle, Right Angle, Bottom Mount, Surface Mount, with Solder Tabs, -30 to 85 degC, 5-Pin USB, RoHS, Tape and Reel	J300	1
TAG connector	nan	J700	1
CON-SMA-EDGE-S	CONN SMA JACK STR EDGE MNT	J1000	1
RMCF0603FT10K0	RES 10K OHM 1% 1/10W 0603	R200, R700	2
ERJ-3EKF22R0V	RES SMD 22 OHM 1% 1/10W 0603	R201, R202, R203, R204, R205	5
1.5 kOhms	RES SMD 1.5K OHM 1% 1/10W 0603	R206	1
0 Ohms	RES 0 OHM JUMPER 1/10W 0603	R207, R208, R703	3
100 kOhms	RES SMD 100K OHM 1% 1/4W 0603	R209	1
CR0603-JW-562ELF	RES SMD 5.6K OHM 5% 1/10W 0603	R300	1
CRCW06031K10FKEA	RES SMD 1.1K OHM 1% 1/10W 0603	R400, R701	2
CRCW060316K0FKEA	RES SMD 16K OHM 1% 1/10W 0603	R600	1
RR0816P-271-D	RES SMD 270 OHM 0.5% 1/16W 0603	R601	1
RMCF0603FT11K0	RES 11K OHM 1% 1/10W 0603	R602	1
RMCF0603JT470R	RES 470 OHM 5% 1/10W 0603	R603, R604, R605, R606	4
560 Ohms	RES 560 OHM 5% 1/10W 0603	R702	1
MIC5219-3.3YM5-TR	IC REG LINEAR 3.3V 500MA SOT23-5	U400	1
TLV75518PDBVR	IC REG LINEAR 1.8V 500MA SOT23-5	U500	1
DW1000-I-TR13	IC RF TXRX 802.15.4 48QFN	U600	1

Continued on next page

Name	Description	Designator(s)	Qty
STM32F103C8T6TR	ARM Cortex-M3 32-bit MCU 64KB Flash 48-Pin LQFP	U700	1
ECS-TXO-20CSMV4-384-AY-TR	Crystal or Oscillator	Y600	1
831066657	831066657 WE-SPXO Crystal Oscillator	Y700	1

IV. Amplifier Schematics

This PCB MUST BE manufactured according to spec JLC04161H-3313
Impedance calculator: https://jlcpcb.com/pcb-impedance-calculator

Impedance (Ω)	Type	Signal Layer	Top Ref	Bottom Ref	Trace Width	Trace Spacing	Impedance trace to copper
50	Single Ended (Non coplanar)	L1	/	L2	0.1565	/	/
50	Differential Pair (Non coplanar)	L1	/	L2	0.4493	0.2032	/

Layer	Material	Thickness (mil)	Thickness (mm)
L1	Outer Copper Weight1oz	1.38	0.0350
Prepreg	3313 RC57% 4.2mil	3.91	0.0994
L2	Inner Copper Weight	0.60	0.0152
Core	1.3mm H/HOZ with copper	49.80	1.2650
L3	Inner Copper Weight	0.60	0.0152
Prepreg	3313 RC57% 4.2mil	3.91	0.0994
L4	Outer Copper Weight1oz	1.38	0.0350

Title		
Size A4	Number	Revision
Date: 4/09/2025		Sheet of
File: C:\Users\..\INDEX.SchDoc		Drawn By:

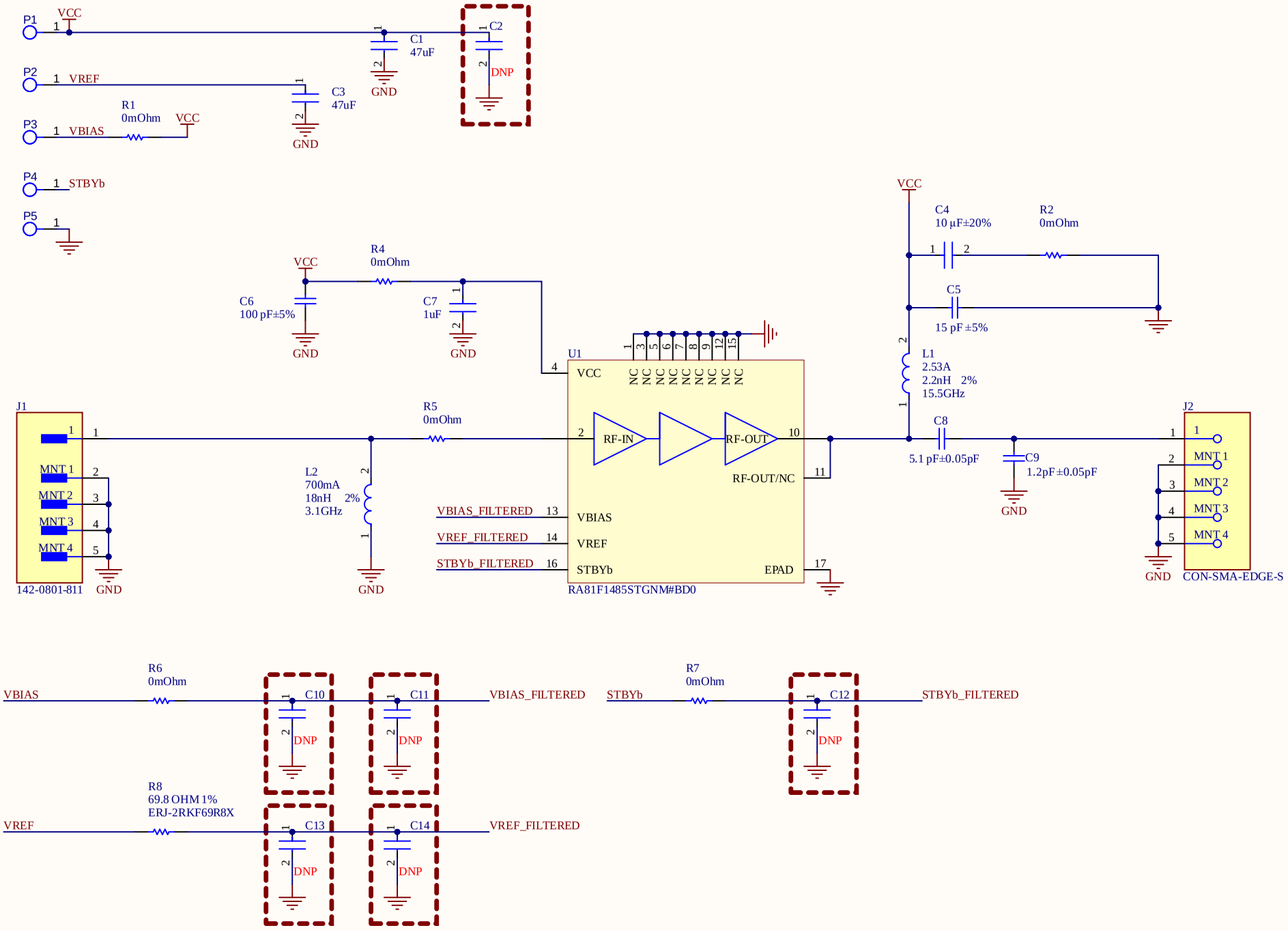
P1
VCC
P2
VREF
P3
VBIAS
R1
0mOhm
VCC
C1
47uF
GND
C2
DNP
C3
47uF
GND
P4
STBYb
P5
VCC
C6
100 pF±5%
GND
R4
0mOhm
C7
1uF
GND
U1
VCC
NC
RF-IN
RF-OUT
RF-OUT/NC
VBIAS
VREF
STBYb
EPAD
VBIAS_FILTERED
VREF_FILTERED
STBYb_FILTERED
RA81F1485STGNM#BD0
VCC
C4
10 µF±20%
R2
0mOhm
C5
15 pF ±5%
L1
2.53A
2.2nH 2%
15.5GHz
C8
5.1 pF±0.05pF
C9
1.2pF±0.05pF
GND
J1
MNT 1
MNT 2
MNT 3
MNT 4
142-0801-811
GND
R5
0mOhm
L2
700mA
18nH 2%
3.1GHz
GND
J2
MNT 1
MNT 2
MNT 3
MNT 4
GND
CON-SMA-EDGE-S
VBIAS
R6
0mOhm
C10
DNP
C11
DNP
VBIAS_FILTERED
STBYb
R7
0mOhm
C12
DNP
STBYb_FILTERED
VREF
R8
69.8 OHM 1%
ERJ-2RKF69R8X
C13
DNP
C14
DNP
VREF_FILTERED

V. Amplifier PCB

Top, Inner 1, Inner 2, Bottom and Overlay layers are shown.

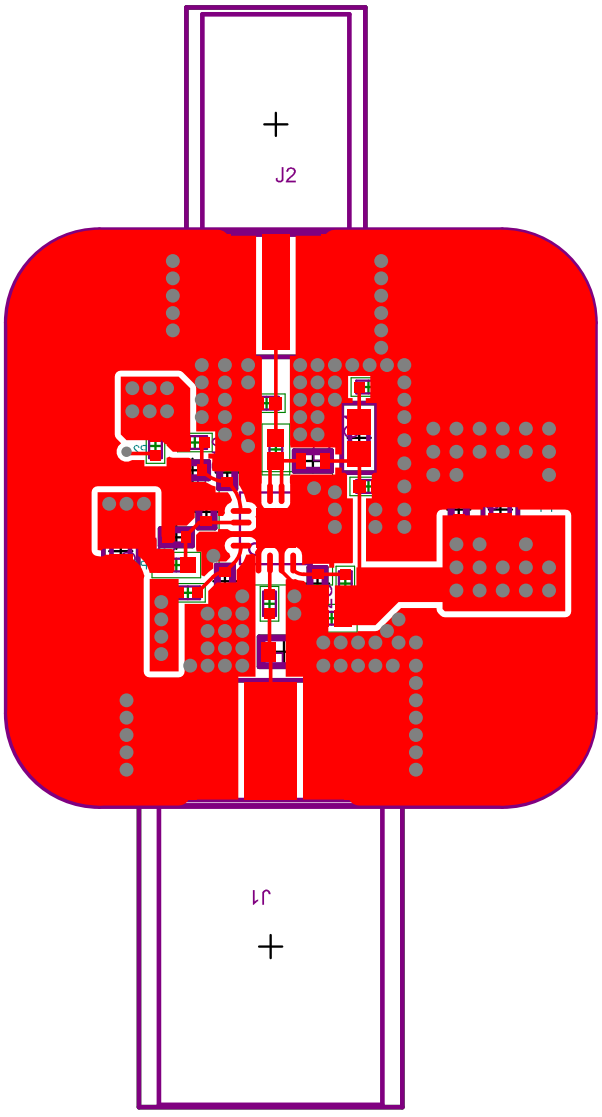
J2
J1

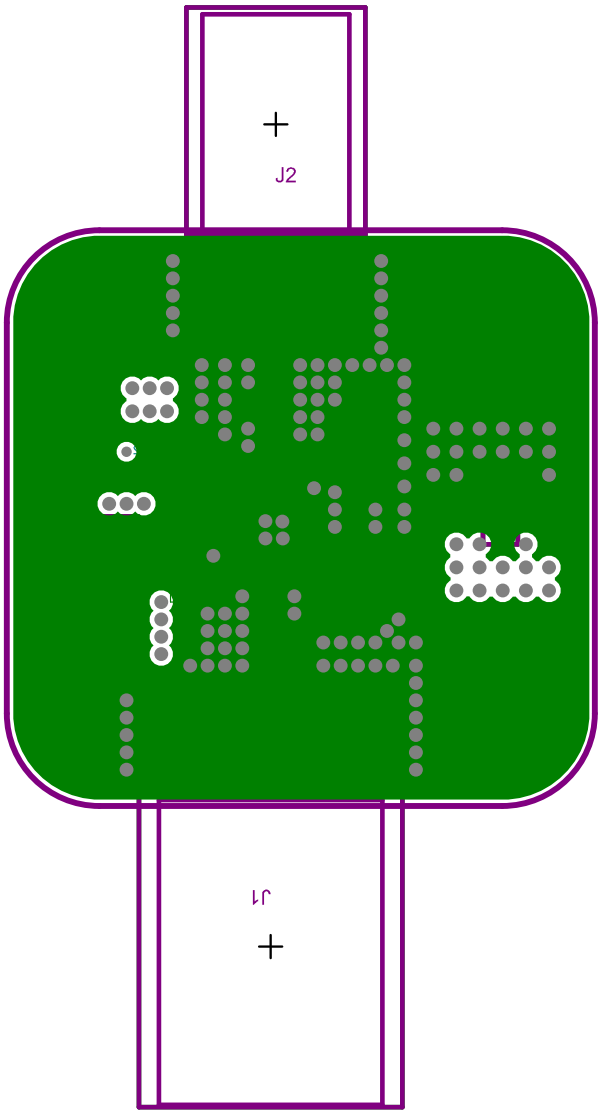
J2
J1

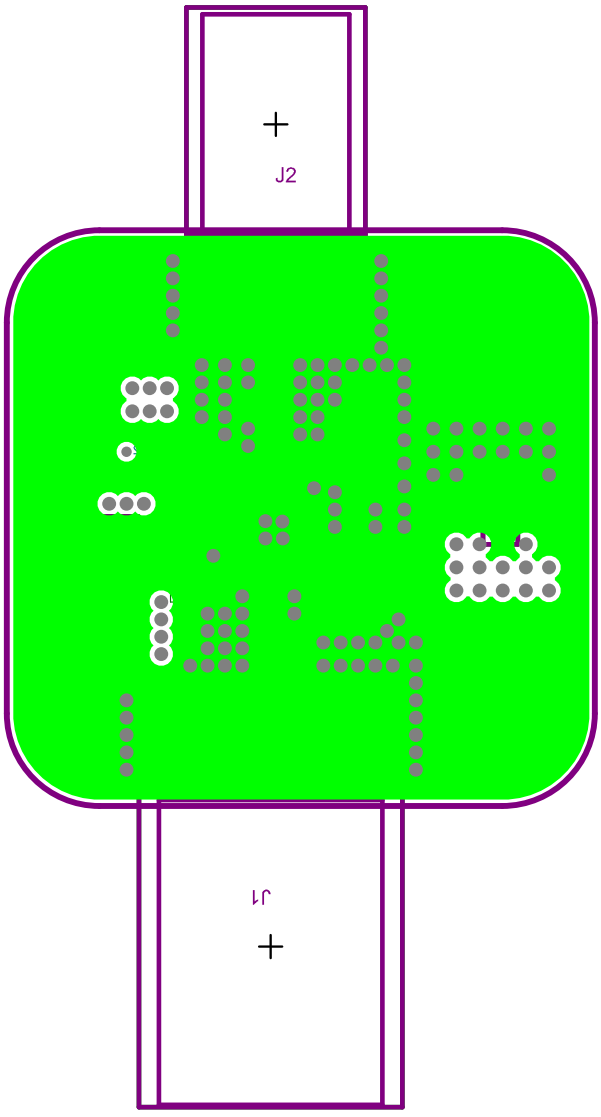
J2
J1

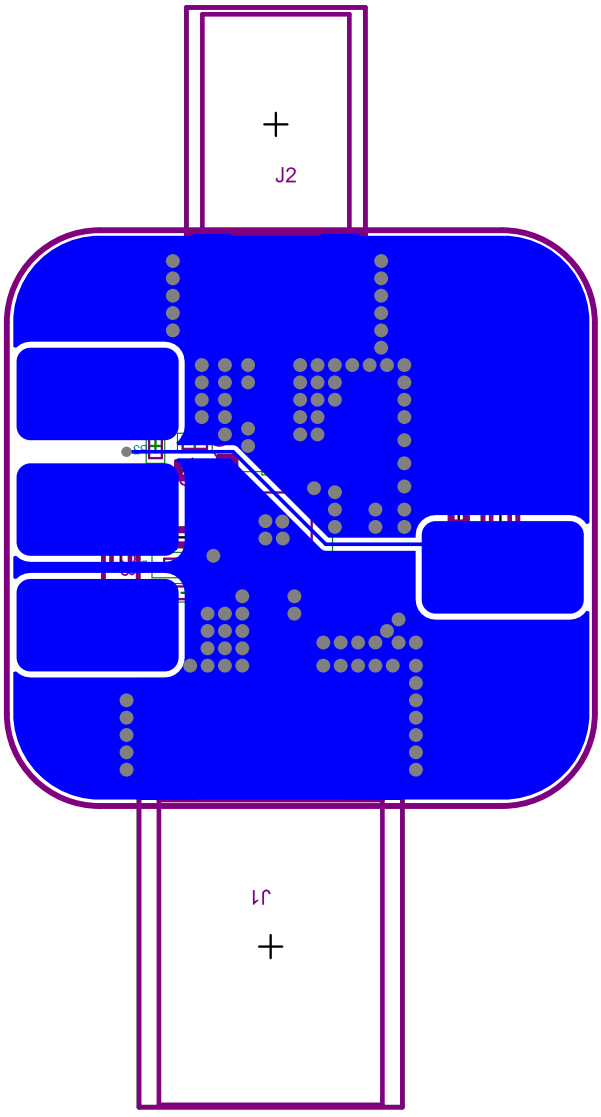
J2
J1

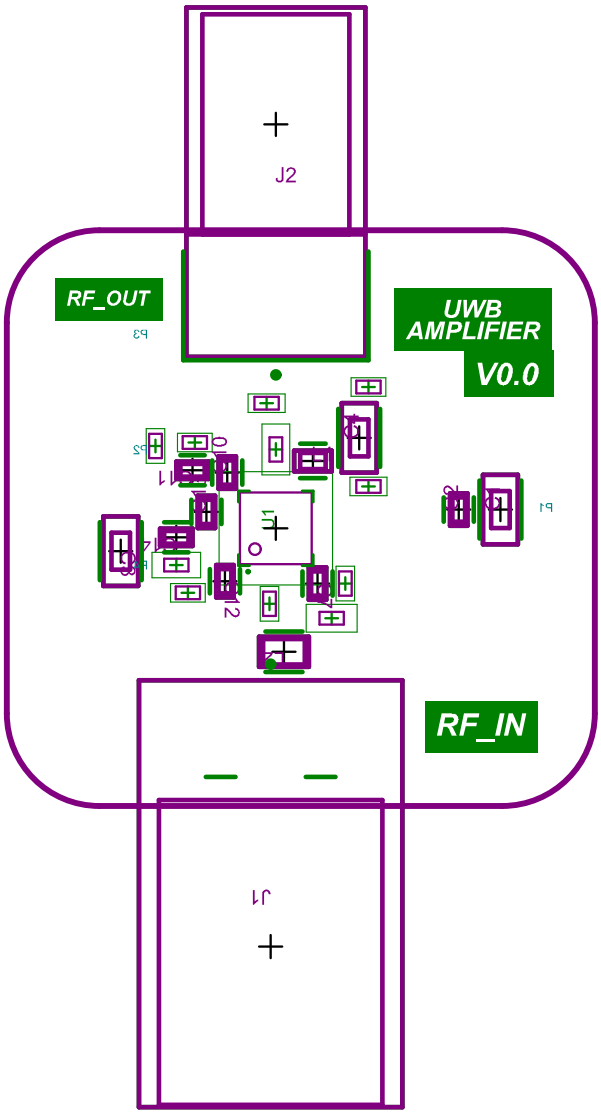
J2
RF_OUT
UWB
AMPLIFIER
V0.0
RF_IN
J1

VI. Amplifier Bill of Materials

Name	Designator(s)	Qty
GRM188R60J476ME15D	C1, C3	2
GRM188Z71A106MA73D	C4	1
GRM1555C1H150JA01D	C5	1
GRM1555C1H101JA01D	C6	1
GRM155C81C105KE11D	C7	1
LQW15AN15NG80D	L1	1
LQW15AN10NG80D	L2	1
MMIC Amplifier	U1	1
Header 1x2	J1	1
SMA Connector	J2	1
SMA Connector	J3	1
0 Ohm Jumper	R1	1

Licence

Non-exclusive licence to reproduce thesis and make thesis public

I, Oliver Vaht,

1. herewith grant the University of Tartu a free permit (non-exclusive licence) to reproduce, for the purpose of preservation, including for adding to the DSpace digital archives until the expiry of the term of copyright,

   Design and Characterization of an Ultra-Wideband Radio for Extended-Range Transmission,

   supervised by Jaanus Kalde.

2. I grant the University of Tartu a permit to make the work specified in p. 1 available to the public via the web environment of the University of Tartu, including via the DSpace digital archives, under the Creative Commons licence CC BY NC ND 3.0, which allows, by giving appropriate credit to the author, to reproduce, distribute the work and communicate it to the public, and prohibits the creation of derivative works and any commercial use of the work until the expiry of the term of copyright.

3. I am aware of the fact that the author retains the rights specified in p. 1 and 2.

4. I certify that granting the non-exclusive licence does not infringe other persons' intellectual property rights or rights arising from the personal data protection legislation.

Oliver Vaht

May 19, 2025